



UNIVERSITY OF NAIROBI

// A DETERMINATION OF THE GEOID OVER NAIROBI AREA //

by

Patroba Achola Odera

UNIVERSITY OF NAIROBI
EAST AFRICANA COLLECTION

A thesis submitted in partial fulfilment for the degree of Master of Science in Surveying in the
University of Nairobi

University of NAIROBI Library



0442396 8

September, 2005

JOMO KENYATTA MEMORIAL
LIBRARY

DECLARATIONS

This thesis is my original work and has not been presented for a degree in any other University



8/9/2005

P.A. Odera

This thesis has been submitted for examination with my approval as University supervisor



08/9/2005

Dr. - Ing. S.M. Musyoka

ABSTRACT

The precise geoid determination is one of the main current geodetic problems in Kenya. This is because Global Positioning System (GPS) defined coordinates require geoid heights so as to be compatible to orthometric heights that are used in practice. The geoid is the reference surface for orthometric heights, which are the functional heights for mapping, engineering works, navigation, and other geophysical applications.

In this study, a local geoid has been determined by geometric approach. The geoid heights are derived from geodetic and orthometric heights. The geodetic and orthometric heights in this study are referred to the World Geodetic System 1984 (WGS84) and the local mean sea level respectively. Nineteen points levelled by both GPS and precise levelling techniques in the area of study have been used.

In order to express the local geoid as a function of the local plane coordinates, it is deemed necessary to determine three-dimensional transformation parameters between WGS84 and Arc-Datum 1960 (local datum). Seven triangulation points have been used for the determination of transformation parameters in the area of study.

The geoid height is expressed as a function of the local plane coordinates through a biquadratic surface polynomial. The coefficients of the biquadratic polynomial are determined by two methods: Least Squares (LS) and Least Squares Collocation (LSC) using 14 GPS/Levelling points. Five points have been used for testing the results. It is found that the coefficients determined by LS and LSC model the geoid at the same level on the test points. However, LSC technique provides stochastic parameters to the predicted geoid heights. Earth Gravity Model of 1996 (EGM96) has also been used to determine geoid heights although it compares poorly at the test points.

The experience with Nairobi area geoid indicates that modelling the geoid by a biquadratic polynomial is simple and it works well. The geoid heights obtained by biquadratic polynomial (determined by LS and LSC) compare favourably on the test points with root mean square and standard deviation of ± 1 cm in the area of study.

A MATLAB program (RUN.M) has been developed to functionalise the use of the transformation parameters and the polynomial. The program interacts with the user through a user interface. From the observed WGS84 coordinates, the local Universal Transverse Mercator (UTM) coordinates (N, E) on Arc-Datum 1960 are computed followed by the interpolation of geoid height and subsequently the orthometric height of a given point within the area of study. The extents of the area of study are: latitudes ($1^{\circ} 8' 00''$ S to $1^{\circ} 25' 18''$ S) and longitudes ($36^{\circ} 38' 55''$ E to $36^{\circ} 58' 24''$ E).

The results show that if geoid heights are accurately determined, then a biquadratic polynomial can be used for geoid modelling. The combination of transformation parameters and biquadratic polynomial is therefore a possible way of enabling the use of GPS for local survey work.

ACKNOWLEDGEMENTS

I wish to express my sincere gratitude to my supervisor, Dr. – Ing. S.M. Musyoka under whose direction this work was done. Helpful discussions, positive criticisms, timely advice and relevant reference materials that he provided contributed enormously towards the successful completion of this thesis.

I would also like to thank the Board of Postgraduate Studies, University of Nairobi, for the financial support that enabled me to pursue this course. I wish to salute the chairman, Faculty Postgraduate Studies Committee, Dr. – Ing. J.B.K. Kiema, for the pieces of advice he gave to me in support of this study.

I am thankful to the Survey of Kenya (technical section) and the Kenya Institute of Surveying and Mapping, for the valuable data provided. My deep appreciation goes to my parents, siblings, relatives and friends who supported me in one way or another throughout my study period.

I am grateful to the chairman, Department of Surveying, Mr. G.O. Wayumba and the former dean, Faculty of Engineering, Dr. G.C. Mulaku, for the enabling environment created and administrative support granted. Similarly I wish to recognize the support of staff and students of the Department of Surveying, for the moral support during the preparation of this thesis. In particular, I am grateful to Mr. A.S. Lwangasi and Prof. F.W.O. Aduol, for their generous technical support.

Finally I am grateful to the Almighty God, for the provision of the necessary spiritual nourishment, good health and knowledge during my studies at the University of Nairobi. For sure only you Lord is worthy to be worshipped.

DEDICATION

This thesis is dedicated to my late father Richard Odera Obong, my mother Rose Atieno Odera and above all the Almighty God.

TABLE OF CONTENTS

| | |
|---|------------|
| DECLARATIONS | ii |
| ABSTRACT | iii |
| ACKNOWLEDGMENTS | v |
| DEDICATION | vi |
| TABLE OF CONTENTS | vii |
| LIST OF FIGURES | x |
| LIST OF TABLES | xi |
| LIST OF ABBREVIATIONS | xii |
| | |
| 1 INTRODUCTION | 1 |
| 1.1 General Background | 1 |
| 1.2 Statement of the Problem | 3 |
| 1.3 Objectives | 4 |
| 1.4 Methodology | 5 |
| 1.5 Organization of the Report | 5 |
| | |
| 2 GEOID DETERMINATION AND MODELLING | 6 |
| 2.1 Geoid Determination Methods | 6 |
| 2.1.1 Astro-geodetic (Astronomic Levelling) | 6 |
| 2.1.2 Geometrical Astronomic Levelling | 7 |
| 2.1.3 Gravimetric Approach | 7 |
| 2.1.4 Satellite Methods | 9 |
| 2.1.4.1 Satellite Perturbed Motion | 9 |
| 2.1.4.2 Satellite Geometric Approach | 10 |
| 2.1.5 Combined Solutions of the Geoid | 11 |
| 2.2 Geoid Modelling | 12 |
| 2.2.1 Least Squares Collocation | 12 |
| 2.2.2 Geopotential Models | 16 |
| 2.2.3 Interpolating Polynomial | 18 |

| | | |
|----------|---|-----------|
| 3 | HEIGHT SYSTEMS AND GLOBAL POSITIONING SYSTEM | 20 |
| 3.1 | Height Systems | 20 |
| 3.1.1 | Orthometric Heights | 20 |
| 3.1.2 | Geodetic Heights | 22 |
| 3.2 | Global Positioning System (GPS) | 23 |
| 3.2.1 | GPS Coordinates | 24 |
| 3.2.2 | Accuracy of GPS Surveying | 26 |
| 4 | LOCAL COORDINATE SYSTEM | 28 |
| 4.1 | Definitions | 28 |
| 4.2 | Arc-Datum 1960 | 29 |
| 4.3 | Universal Transverse Mercator (UTM) Coordinate System | 30 |
| 4.3.1 | UTM Grid Coordinates | 30 |
| 4.3.2 | UTM Mapping Equations | 31 |
| 4.3.3 | Grid to Geodetic Conversion and vice versa | 33 |
| 5 | COORDINATE TRANSFORMATIONS | 35 |
| 5.1 | Introduction | 35 |
| 5.2 | Transformation between Cartesian and Geodetic Coordinates | 35 |
| 5.3 | Datum Transformation | 37 |
| 5.3.1 | Three Dimensional Transformation | 37 |
| 5.3.1.1 | Rotation Matrices | 38 |
| 5.3.1.2 | Bursa–Wolf Model | 40 |
| 5.3.1.3 | Molodensky Model | 40 |
| 5.4 | Estimation Model | 41 |
| 5.5 | Accuracy Estimation | 42 |
| 6 | TEST DATA AND COMPUTATIONS | 43 |
| 6.1 | Triangulation Stations | 43 |
| 6.2 | WGS84 and Arc– Datum 1960 Coordinates | 44 |
| 6.3 | Determination of Transformation Parameters | 47 |
| 6.4 | GPS/Levelling Points | 48 |

| | | | |
|----------|-------|--|-----------|
| | 6.5 | Polynomial Determination | 51 |
| | 6.5.1 | Determination of Coefficients by Least Squares | 53 |
| | 6.5.2 | Determination of Coefficients by Least Squares Collocation | 53 |
| | 6.6 | Interpolation of Geoid Heights | 54 |
| 7 | | RESULTS AND ANALYSIS | 55 |
| | 7.1 | Transformation Parameters | 55 |
| | 7.2 | Polynomial Coefficients by Least Squares | 55 |
| | 7.2.1 | Application of Polynomial Coefficients by LS on Test Data | 56 |
| | 7.3 | Polynomial Coefficients by Least Squares Collocation | 56 |
| | 7.3.1 | Application of Polynomial Coefficients by LSC on Test Data | 57 |
| | 7.4 | Application of EGM96 on Test Data | 57 |
| | 7.5 | The Nairobi Area Geoid | 57 |
| | 7.6 | Analysis | 59 |
| 8 | | CONCLUSIONS AND RECOMMENDATIONS | 62 |
| | 8.1 | Conclusions | 62 |
| | 8.2 | Recommendations | 63 |
| | | APPENDICES | 65 |
| | A. | Preliminary Program | 65 |
| | B. | Main Program | 67 |
| | C. | User Interface | 81 |
| | | REFERENCES | 83 |

LIST OF FIGURES

| | | |
|-----------------|---|----|
| Figure 1.2.1: | Relationship between geoid and reference ellipsoid | 3 |
| Figure 3.1.1.1: | Orthometric height | 20 |
| Figure 3.1.2.1: | Geodetic height | 23 |
| Figure 3.2.1.1: | Cartesian and geodetic coordinates | 24 |
| Figure 6.1.1: | Spatial distribution of the triangulation points | 43 |
| Figure 6.3.1: | Flow chart showing determination of seven transformation parameters | 48 |
| Figure 6.4.1: | Spatial distribution of the GPS/Lev points within the triangulation network | 51 |
| Figure 6.5.1: | Flow chart showing determination of the coefficients of the polynomial | 52 |
| Figure 6.6.1: | Flow chart showing interpolation of geoid heights | 54 |
| Figure 7.5.1: | Nairobi area geoid | 58 |

LIST OF FIGURES

| | | |
|-----------------|---|----|
| Figure 1.2.1: | Relationship between geoid and reference ellipsoid | 3 |
| Figure 3.1.1.1: | Orthometric height | 20 |
| Figure 3.1.2.1: | Geodetic height | 23 |
| Figure 3.2.1.1: | Cartesian and geodetic coordinates | 24 |
| Figure 6.1.1: | Spatial distribution of the triangulation points | 43 |
| Figure 6.3.1: | Flow chart showing determination of seven transformation parameters | 48 |
| Figure 6.4.1: | Spatial distribution of the GPS/Lev points within the triangulation network | 51 |
| Figure 6.5.1: | Flow chart showing determination of the coefficients of the polynomial | 52 |
| Figure 6.6.1: | Flow chart showing interpolation of geoid heights | 54 |
| Figure 7.5.1: | Nairobi area geoid | 58 |

LIST OF TABLES

| | | |
|----------------|---|----|
| Table 6.1.1: | Description of the triangulation points | 43 |
| Table 6.2.1: | WGS84 ellipsoidal curvilinear coordinates of the triangulation points | 45 |
| Table 6.2.2: | WGS84 ellipsoidal cartesian coordinates of the triangulation points | 45 |
| Table 6.2.3: | Local UTM plane coordinates and orthometric heights of the triangulation points | 46 |
| Table 6.2.4: | Local geodetic coordinates of the triangulation points | 46 |
| Table 6.2.5: | Local ellipsoidal cartesian coordinates of the triangulation points | 47 |
| Table 6.4.1: | GPS coordinates (geodetic: - latitudes and longitudes) of the GPS/Lev points | 49 |
| Table 6.4.2: | Geodetic heights, orthometric heights and geoidal undulations of the GPS/Lev points | 50 |
| Table 7.1.1: | Transformation parameters | 55 |
| Table 7.2.1: | Coefficients by Least Squares | 55 |
| Table 7.2.1.1: | Interpolated geoid heights by polynomial (LS) at the test points | 56 |
| Table 7.3.1: | Coefficients by Least Squares Collocation | 56 |
| Table 7.3.1.1: | Interpolated geoid heights by polynomial (LSC) at the test points | 57 |
| Table 7.4.1: | Interpolated geoid heights by EGM96 at the test points | 57 |
| Table 7.6.1: | Residuals obtained by LS and LSC at the data points | 59 |
| Table 7.6.2: | Differences of geoid heights | 60 |

LIST OF ABBREVIATIONS

| | |
|---------|--|
| BIH | Bureau International del' Heure |
| CIO | Conventional International Origin |
| Cov | Covariance |
| CTP | Conventional Terrestrial Pole |
| DMA | Defence Mapping Agency |
| DOS | Directorate of Overseas Surveys |
| EGM96 | Earth Gravity Model 1996 |
| GDOP | Geometric Dilution of Precision |
| GLONASS | Global' naya Navigationaya Sputnikovaya Sistema – Global Navigation Satellite System |
| GMM | Gauss Markov Model |
| GPS | Global Positioning System |
| GSFC | Goddard Space Flight Centre |
| IAG | International Association of Geodesy |
| IERS | International Earth Rotation Service |
| IUGG | International Union of Geodesy and Geophysics |
| LC | Least Squares |
| LSC | Least Squares Collocation |
| Lev | Levelling |
| NASA | National Aeronautics and Space Administration |
| NATO | North Atlantic Treaty Organization |
| NAVSTAR | Navigation System with Timing and Ranging |
| NIMA | National Imagery and Mapping Agency |
| NSWC | Naval Surface Warfare Centre |
| OSU91 | Ohio State University 1991 |
| PDOP | Position Dilution of Precision |
| PPS | Precise Positioning Service |
| RMS | Root Mean Square |
| SPS | Standard Positioning Service |
| UTM | Universal Transverse Mercator |
| WGS84 | World Geodetic System 1984 |

CHAPTER ONE

INTRODUCTION

1.1 General Background

The geoid may be defined as the one gravity equipotential surface that best approximates the idealized mean sea level over the whole earth. This surface was already referred to by *Carl Friedrich Gauss (1777 –1855)* as the mathematical form of the earth and later named geoid by *J.B. Listing (1873)*. The geoid can be viewed as a surface of constant potential, $W_{(x, y, z)} = W_0$, where “W” is the earth’s gravity potential and “W₀” is the geoid potential as specified by the International Association of Geodesy (*Moritz, 1980*). If we consider the waters of the oceans as freely moving homogeneous matter, which is subject only to the force of gravity of the earth, then upon attaining a state of equilibrium, the surface of such idealized oceans assume a level surface of the gravity field – extended under the continents (*Torge, 1991*). Thus the geoid is a closed and continuous level surface, which extends inside the solid body of the earth.

The curvature of the geoid displays discontinuities at abrupt density variations and consequently it is not an analytic surface to be suited as a reference surface for position determinations (*Torge, 1980*). It is well suited as a reference surface for potential or height differences (levelling combined with gravity measurements). To establish the geoid, one utilizes the mean sea level, which may deviate by about $\pm 1\text{m}$ to $\pm 2\text{m}$ from a level surface. The deviation is due to; ocean tides, meteorological nature of pressure and winds, oceanographic nature of currents, density differences in ocean waters (due to temperature and salinity), and water bulges of melt water and monsoon rains.

For better accuracies ($\pm 10\text{ cm}$) the above classical definition of the geoid (as mean sea level and its extension) is not sufficient. The accuracy attainable through possibilities of satellite geodesy requires the geoid to be defined as a global reference surface (for heights) which best fits the mean sea level, i.e. the potential and elevation of the geoid are obtained by applying a minimum condition for deviations between the geoid and the mean sea level.

The method of using mean sea level as the reference surface for orthometric height has been widely acceptable. However, *Rizos (1980)* observed that the mean value of the local mean sea level observed at the tide gauge stations cannot be considered to coincide with the geoid. This therefore means that a mean sea level at one position is not on the same

geopotential surface as that at another position. The use of mean sea level as reference surface may cause some problems in vertical-datum application. The first problem is related to the use of multiple constraints on mean sea levels in a single vertical datum. In such a case, heights at tide gauge sites are set to be zero in the levelling adjustments (*Pan and Sjöberg, 1998*). The other problem is that the deviation of the mean sea level from the geoid is of the order of $\pm 2\text{m}$ (*Rapp and Balasubramania, 1992*), which implies that various height systems based on fixing tide gauges may differ by the same order.

The shape of the mean sea level is determined from records of the instantaneous sea level at a chain of observational points located on coastlines and equipped with tide gauges. These data from all over the world are received at the headquarters of the Permanent Service for Mean Sea Level (PSMSL) at the Bilston Observatory (*Cheshire, U.K*) for worldwide dissemination.

In essence mean sea level determined rigorously is the geoid. The geoid represents the most obvious mathematical formulation of a horizontal surface at sea level. This is why the use of the geoid simplifies geodetic problems and makes them accessible to geometrical intuition (*Heiskanen and Moritz, 1967*). The height datum is achieved by determining the mean sea level on the seashore. The mean sea level is believed to deviate from the location of the geoid by negligible amounts. To use the mean sea level to provide orthometric heights, a tide-gauge station is set up at the sea and next to it is set a reference benchmark (Ref.BM) i.e. a height datum on firm ground.

In geodetic positioning the geoid is approximated with a rotational ellipsoid (with semi-minor axis perpendicular to the equatorial plane) as conventional reference surface. This reference ellipsoid through its deviations from the geoid, further serves as a means of describing the geoid. The components of these deviations are generally known as deflection of the vertical and geoid undulation. The two components are referred to as geoidal deviations. Unlike the topographic surface, which departs from the ellipsoid by several kilometers at slopes of almost any amount, the geoid scarcely deviates from the ellipsoid by as much as a hundred meters, at slopes rarely exceeding one minute of an arc (*Magnavox Research Laboratory Report, 1972*).

1.2 Statement of the Problem

Geodesists have for a long time carried out extensive work geared towards the determination of the geoid. A mathematical figure (ellipsoid of revolution) has been used to represent the earth for mapping purposes. To express the true relationship of points on the earth surface to each other or to the earth's center of mass, the separation between the geoid and the adopted reference ellipsoid must be known. Figure 1.2.1 below shows the relationship between the geoid and the reference ellipsoid.

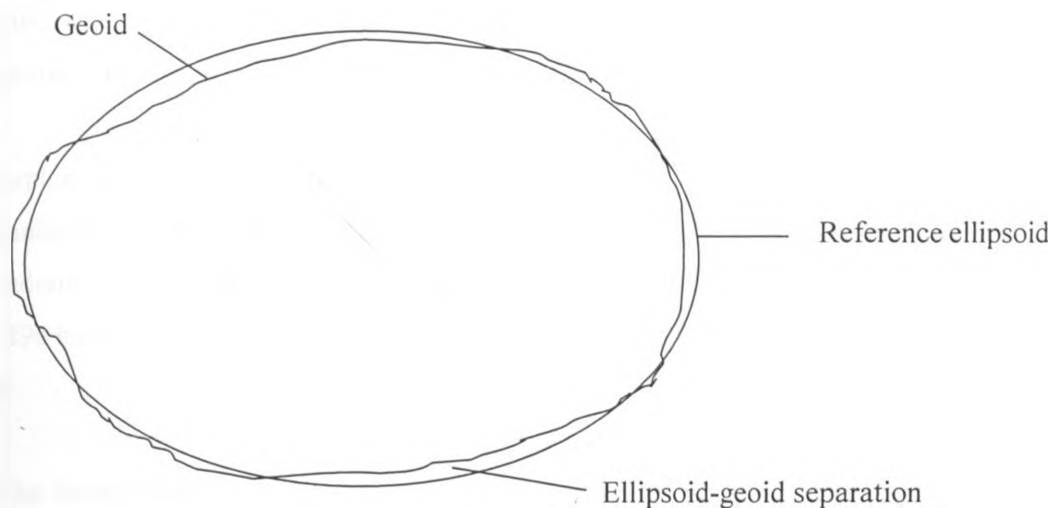


Figure 1.2.1: Relationship between geoid and reference ellipsoid

The linear difference between the reference ellipsoid and the geoid at a point is referred to as geoidal undulation. Determination of the geoid therefore refers to the determination of geoidal undulation (N) from a reference ellipsoid (WGS84 in this case). The knowledge of geoid is normally required principally for practical purposes e.g. surveying, cartography, navigation, determination of the orbit of the artificial satellites, study of the earth's crust and other geophysical studies.

Both gravimetric and geometric methods have been used for geoid determination in various countries e.g. Turkey, Canada, Hong Kong, Belgium, Japan and many other countries. Even though local geoid is very important for the development of a country, no serious attempt has ever been made to determine the geoid for Kenya. Gravity observations in Kenya began around 1955 and observations have been carried out by various organizations, notably petroleum companies (*Lwangasi, 1991*). These data are unfortunately scanty in format and distribution in addition to being not readily available for research work especially in Nairobi

area where less or no exploration activities have been done. Hence the geometric geoid determination approach.

GPS is a new technology in surveying. It is fast and efficient in determination of positional data (coordinates) based on the WGS84. It measures heights above WGS84 reference ellipsoid. These heights are called ellipsoidal heights (h). However orthometric heights (H) are the functional heights for mapping, engineering works, navigation, and other geophysical applications (Ayhan, 1993). The geoid is the reference surface for orthometric heights. These heights are obtained via spirit levelling which is a very tedious and expensive process.

To exploit the capabilities of GPS for heighting purposes, the geoidal undulations must be determined in an area. In this case, Nairobi province has been chosen as the study area. A biquadratic polynomial (determined by LS and LSC) and a gridded representation of EGM96 have been used to convert ellipsoidal heights into orthometric heights in the area of study.

For the interpolated geoid heights to be used effectively for local work, their positions should be known in the local coordinate system. This therefore calls for the determination of transformation parameters between WGS84 and the local (Arc-Datum 1960) coordinates. It is therefore necessary that the geoid height be expressed as a function of the local coordinates (x, y).

1.3 Objectives of the Study

The objectives of this study include,

- (i) Determination of the geoid in Nairobi area.
- (ii) Determination of transformation parameters between WGS84 and Arc - Datum 1960 (Local) coordinates in the area of study.
- (iii) Determination of a best fitting polynomial expressing the geoidal undulation as a function of the plane coordinates in the area of study.
- (iv) Developing a computer program for converting GPS heights (h) into orthometric heights (H) in the area of study.

1.4 Methodology

A network of seven triangulation points in Nairobi area has been used to determine transformation parameters. The local plane (UTM) coordinates are first transformed to geodetic coordinates. The geodetic coordinates are then used to determine three-dimensional cartesian coordinates based on Arc-Datum 1960 together with the dimensions of modified Clarke 1880 reference ellipsoid.

The corresponding three-dimensional cartesian coordinates on WGS84 complete the requirement for a set of coordinates for every point in the two systems. Three dimensional transformation equations are then used to determine the seven transformation parameters.

A geometric approach has been used for the determination of geoid height i.e. through ellipsoidal and orthometric heights in the area of study. The geoid has been modelled by biquadratic polynomial determined by LS and LSC techniques. A gridded representation of EGM96 has also been used to determine geoid heights through a bilinear interpolation program INTPT.F.

1.5 Organization of the Report

Following this introduction is chapter two which gives the theoretical aspects of geoid determination and modelling. The height systems used in the study and global positioning system are discussed in chapter three. The local coordinate system is discussed in chapter four followed by the various coordinate transformations and parameter estimation models in chapter five.

The test data used in this study and the computations are presented in chapter six while chapter seven is dedicated to results and analysis. Conclusions and recommendations are given in chapter eight. The appendices and references are presented in that order immediately after chapter eight. The computer programs used in the study are given in the appendices.

CHAPTER TWO

GEOID DETERMINATION AND MODELLING

2.1 Geoid Determination Methods

The geoid is basically the physical surface of the earth. This surface can be determined via different methods: Astro-geodetic (Astronomic Levelling), Geometrical Astronomical Levelling, Gravimetric and Satellite methods. Better determination of the geoid may be obtained by combined evaluation. The most common combinations are; Astro – Gravimetric Levelling and Gravimetric – Satellite solution (*Heiskanen and Moritz, 1967*).

2.1.1 Astro-Geodetic (Astronomic Levelling)

In Astro - geodetic method we consider the problem of determination of the figure of the earth by use of astronomic and terrestrial geodetic methods. The data derived from the astronomic and terrestrial geodetic observations are the deflection of the vertical parameters, which imply the slope of the geoid with respect to the reference ellipsoid, so that from this relationship the geoidal height differences are determined. This can be given as.

$$dN = -\theta ds \quad (2.1.1-1)$$

where,

dN is the geoid height difference,

ds is differential change in horizontal distance,

and

θ is the total deflection of the vertical given as,

$$\theta = \xi \cos \alpha_{AB} + \eta \sin \alpha_{AB} \quad \text{for a line AB} \quad (2.1.1-2)$$

where,

ξ is the deflection of the vertical in the meridian direction,

η is the deflection of the vertical in the prime vertical direction ,

α_{AB} is azimuth from point A to B.

The difference in geoid height may also be given as,

$$dN = N_B - N_A = - \int_A^B \theta ds = - \int (\xi \cos \alpha_{AB} + \eta \sin \alpha_{AB}) ds = - \sum_{l=1}^n \theta_l ds. \quad (2.1.1-3)$$

2.1.2 Geometrical Astronomic Levelling

In the geometric astronomical levelling, geometrical levelling is combined with the astro-geodetic data and is often incorporated into three-dimensional computations. The difference in geoidal undulation is obtained from the relationship;

$$dh = dn + dE + dN. \quad (2.1.2-1)$$

where,

- dh is geodetic height difference,
- dh is orthometric height difference,
- dN is geoid height difference,
- dE is orthometric height correction,
- dn is levelled height difference.

Hence for a line AB, Δh_{AB} is given as

$$\Delta h_{AB} = h_B - h_A = \int_A^B dn - \int_A^B \theta ds. \quad (2.1.2-2)$$

where,

Δh_{AB} is the geodetic height difference between points (A and B).

Eqn (2.1.2-3) shows that the difference in geodetic height can be obtained using levelling and the surface deflections of the vertical. With parallelism of axes of the geodetic (x, y, z) and astronomic (X, Y, Z) systems we have that;

$$d(\Delta h_{AB}) = \cos \phi_B \cos \lambda_B dX_B - \cos \phi_A \cos \lambda_A dX_A + \cos \phi_B \cos \lambda_B dY_B - \cos \phi_A \cos \lambda_A dY_A + \sin \phi_B dZ_B - \sin \phi_A dZ_A. \quad (2.1.2-3)$$

where,

- ϕ is geodetic latitude,
- λ is geodetic longitude.

2.1.3 Gravimetric Approach

The gravimetric determination of the geoid is based on the solution of the geodetic boundary value problem for the disturbing potential (T). The disturbing potential gives the irregularities of the actual potential (W) from the modelled potential (U) of the figure of the earth. Known boundary-values (gravity anomalies) on the geoid are related to the

disturbing potential in the gravimetric determination of the geoid. The solution to the problem is sought using approaches given by *Stokes's and Molodensky's* concepts, with *Stokes's* approach being the most commonly used method. The disturbing potential (T) satisfies *Laplace's* equation i.e. (*Moritz, 1980; Heiskanen and Moritz, 1967*).

$$\nabla^2 T = \Delta T = \frac{\partial^2 T}{\partial X^2} + \frac{\partial^2 T}{\partial Y^2} + \frac{\partial^2 T}{\partial Z^2} = 0. \quad (2.1.3-1)$$

After evaluating the value of T, the geoidal undulation can be obtained via the *Brun's* formula given by *Heiskanen and Moritz (1967)* as;

$$N = \frac{T}{\gamma}. \quad (2.1.3-2)$$

where,

γ is normal gravity.

In the classical gravimetric approach, T may be obtained as (*Heiskanen and Moritz, 1967*);

$$T(\theta, \lambda) = \frac{GM}{r} \sum_{n=2}^{\infty} \sum_{m=0}^n \left(\frac{a}{r}\right)^n [\delta C_{nm} \cos m\lambda + \delta S_{nm} \sin m\lambda] P_{nm}(\cos \theta). \quad (2.1.3-3)$$

where,

T (θ, λ) is disturbing potential at point (θ, λ) with θ being co - latitude,

a is semi-major axis of a reference ellipsoid,

$P_{nm}(\cos \theta)$ is Legendre polynomial,

n is degree of polynomial coefficients,

m is order of polynomial coefficients.

The coefficients δC_{nm} and δS_{nm} are obtained as the modified harmonic coefficients for the earth (geoid) and the selected geocentric ellipsoid. Substituting for T from (2.1.3-3) into (2.1.3-2) we obtain N (*Heiskanen and Moritz, 1967*) as;

$$N(\theta, \lambda) = R \sum_{n=2}^{\infty} \sum_{m=0}^n [\delta C_{nm} \cos m\lambda + \delta S_{nm} \sin m\lambda] P_{nm}(\cos \theta). \quad (2.1.3-4)$$

Thus with the harmonic coefficients computed, gravimetric geoid height can be evaluated.

The value of N is also given by *Stokes's* formula as;

$$N = \frac{R}{4\pi\gamma_m} \iint_{\sigma} S(\psi) \Delta g d\sigma. \quad (2.1.3-5)$$

where,

$S(\psi)$ is Stokes's function (*Heiskanen and Moritz, 1967*),

R is mean radius of the earth,

Δg is gravity anomaly,

$d\sigma$ is surface element.

2.1.4 Satellite Methods

In satellite determination we use observations to and from artificial satellites. The methods used can be classified into dynamic and geometric. In the dynamic method, the satellite is taken as a sensor moving in/under the gravitational field of the earth from which the perturbation theory can be modelled.

2.1.4.1 Satellite Perturbed Motion

The variation in the orbit of the satellite is caused by various disturbing forces (gravitational and non gravitational). These (disturbing forces) cause variations with time in the orbital elements (orbital perturbations) of secular and long / short periodic nature. The differences are referred to as **perturbations** of the satellite orbit and can be viewed from two different aspects; the coordinates of the satellite are directly disturbed or changed, for which analyses are made to obtain the differences and in the other aspect it is assumed that the satellite is moving in an elliptic orbit whose elements change at each instant and analyses of the changes made.

The causes of perturbations are usually modelled in the form of disturbing functions (R_1), which are to be related to the potential function of the spherical attraction. Hence the potential is given as,

$$W = \frac{GM}{r} + R_1. \quad (2.1.4.1-1)$$

in which R_1 is the perturbing potential containing the harmonic coefficients J_n, C_{nm} and S_{nm} of the harmonic expansion of gravity potential (V), i.e.

$$R_l = -\frac{GM}{r} \sum_{n=2}^{\infty} \left(\frac{a_c}{r}\right)^{n+1} \left[J_n P_n(\cos \theta) + \sum_{m=1}^n \{C_{nm} \cos m\lambda + S_{nm} \sin m\lambda\} P_{nm}(\cos \theta) \right]. \quad (2.1.4.1-2)$$

The solution for the perturbing force involve a determination of the unknown orbital parameters (or deviations of the predicted orbit parameters) and the disturbing gravitations and non-gravitational forces. This may include a large number (infinity, ∞) of the unknown harmonic coefficients. To make the solution easy, usually a number of the unknowns are eliminated before the adjustment. With the harmonic coefficients determined the geoidal undulation (N) is given as,

$$N = -R_{nl} \sum_{n=2}^{n_{\max}} \sum_{m=0}^n [(J_{nm} - J_{nm}^N) \cos m\lambda + K_{nm} \sin m\lambda] P_{nm}(\cos \theta). \quad (2.1.4.1-3)$$

where,

- n_{\max} is the highest degree of coefficients determination,
- J_{nm} and K_{nm} are spherical harmonic potential coefficients,
- J_{nm}^N is normal spherical harmonic potential coefficient.

2.1.4.2 Satellite Geometric Approach

In the satellite geometrical methods, the satellite is regarded as a high flying object whose orbit can be determined and such information used to compute the coordinates of the ground stations (*Vaniček, 1973*). The first technique for satellite positioning was GLONASS followed by the current Global Positioning System. A third generation of satellite systems (GALILEO) is in its development stage. Global Positioning System has been used in this work hence discussed in details in chapter three.

With the development of GPS positioning technique, great attention has been paid to the precise determination of local/regional geoid with an aim to replace the spirit levelling with GPS surveys. In a relatively small and flat area the local geoid can be determined by a combination of GPS derived heights and levelled heights, called the geometric approach (*Yang and Chen, 2002*). A plane or low order polynomial is usually used to model the geoid (*Featherstone et. al 1998*).

The geometric geoid may be obtained as:

$$N = h - H. \quad (2.1.4.2-1)$$

where h and H are the ellipsoidal and orthometric heights respectively while N is the geoidal undulation. Another method of computing the local geoid is by incorporating the geopotential model and local terrain information (*Doerflinger et.al, 1997; Yang and Chen, 1999*). This approach is similar to the remove – restore technique used in the determination of gravimetric geoid. In this method the geoid height N is expressed as:

$$N = N_{GM} + N_I + N_T. \quad (2.1.4.2-2)$$

Where N_{GM} is long wavelength component computed from a geopotential model (e.g. EGM96), N_T is terrain correction evaluated from topographic information (e.g. DTM), and N_I is medium wavelength component obtained by an interpolation/interpretation technique. This refined geometric approach was used to construct the Hong Kong geoid (*Yang and Chen 2002*).

2.1.5 Combined Solutions of the Geoid

The methods of evaluating the geoid can be classified into three broad categories; astro-geodetic, gravimetric and satellite methods. A more detailed classification gives the methods as; conventional satellite techniques, satellite-to-satellite tracking, satellite gradiometry, satellite altimetry, aerial gradiometry, gravimetry and astro-geodesy.

Considering the characteristics of the three broad categories, with the possibilities that all the data needed for a given area may not be available, it is necessary that an optimal solution be obtained by either combining various solutions or combining different data sets for a determination. There are several possibilities of effectively combining the heterogeneous data sets. However, there are two popular/common combinations given below.

- Astro-Gravimetric Levelling (combination of astro-geodetic and gravimetric approaches).
- Gravimetric-Satellite solutions (combination of gravimetric and satellite methods).

2.2 Geoid Modelling

Many surface-modeling techniques can be used for interpolating geoidal deviations. These may include but not limited to; inverse distance to a power, Kriging, minimum curvature, nearest neighbour, polynomial surface fitting, radial basis function, Shepard's methods, least squares collocation and geopotential models, just to mention a few. The choice of a technique to use for modelling the geoid would depend on; accuracy, practicability, serviceability among other factors. In this research however, a biquadratic polynomial determined by LS and LSC has been used. A gridded representation of EGM96 has also been used to determine geoid height through a bilinear interpolation program INTPT.F.

2.2.1 Least Squares Collocation

Least squares collocation is a general method for least squares adjustment that combines prediction and parameter determination process. In geodetic computations, least squares collocation combines the calculation of station coordinates and other orientation parameters (harmonic coefficients, earth orientation parameters, calibration and drift coefficients etc) with the estimation of gravity field quantities of the unsurveyed points, utilizing many types of observables (*Krarpup 1969, Moritz 1973*). Although the least squares collocation is time consuming, and requires additional pre-processing for the covariance function, it offers the possibility of combining data from heterogeneous sources related to the gravity field. Most of the other methods do not provide this important advantage (*Lachapelle and Tscherning 1978; Schwarz and Sideris 1985; Denker et al. 1986; Süinkel et al. 1987; Vanicek and Klausberg 1987; Arabelos 1989; Yang and Chen 2002*).

From the conventional model in Least Squares adjustment we have that;

$$y = AX + \varepsilon. \tag{2.2.1-1}$$

where;

y is vector for n observations,

X is vector for u unknowns,

A is design matrix,

ε is vector of observational errors.

Equation (2.2.1-1) can be generalized to,

$$\mathbf{y} = \mathbf{AX} + \mathbf{s} + \boldsymbol{\varepsilon}. \quad (2.2.1-2)$$

where, \mathbf{s} (signal) is a random quantity in addition to the noise in the observation \mathbf{y} (Moritz 1980) so that the measurement \mathbf{y} consists of a systematic part \mathbf{AX} and two random parts, \mathbf{s} and $\boldsymbol{\varepsilon}$.

Least Squares Collocation furnishes the parameters (\mathbf{X}) by optimally removing the measuring errors, but in addition allowing for the computation of signals at unsurveyed points (prediction). In applying the Least Squares condition of adjustment procedure to both signal and the noise quantities, the problem can be interpreted as an adjustment of condition equations with unknown parameters (Moritz 1980).

In application to global geodesy, the vector of the observations \mathbf{y} contains all the measured quantities. Disregarding the noise, which can be added easily, these quantities may be decomposed into systematic and irregular parts. The systematic part \mathbf{AX} comprises the parameters of the ellipsoidal reference system and the station coordinates. Other systematic effects, such as instrument constants and drift parameters can also be included in the model. The random part consists of the departures of the earth's gravity field from the reference ellipsoid; i.e. the deflections of the vertical, the geoidal undulations, the gravity anomalies and the differences between the harmonic coefficients of the actual and normal gravity field.

The basic equation of LSC is given as,

$$\mathbf{y} = \mathbf{AX} + \mathbf{z}. \quad (2.2.1-3)$$

with $\mathbf{z} = \mathbf{s}' + \boldsymbol{\varepsilon}$; where \mathbf{s}' and $\boldsymbol{\varepsilon}$ vectors are purely random, whose expectation is zero.

If we wish to estimate the signal at an arbitrary number of computation points which may be different from the number of points in the data, we shall have p computation points, so that the signal vector to be computed is \mathbf{p} -vector, $\mathbf{s} = [s_1, s_2, s_3, \dots, s_p]^T$. We can combine this with the vector $\mathbf{z} = [z_1, z_2, z_3, \dots, z_n]^T$ to have,

$$\mathbf{r} = [s_1, s_2, \dots, s_p, z_1, z_2, \dots, z_n]^T = [\mathbf{s}^T, \mathbf{z}^T]^T. \quad (2.2.1-4)$$

the r-vector has a covariance Q given as,

$$Q = \begin{bmatrix} C_{ss} & C_{sy} \\ C_{ys} & C_{yy} \end{bmatrix}, \quad (2.2.1-5)$$

where,

C_{ss} denotes the covariance of the signal, s,

C_{yy} denotes the covariance of the measurement, y,

C_{sy} denotes the cross covariances between s and y.

It should be noted that $E(y) = AX$ from (2.2.1-3) since $E(z) = 0$. If we denote the covariance matrices of vectors s' , ϵ and y as; $C_{s's'} = C$; $C_{\epsilon\epsilon} = D$ and $C_{yy} = \bar{C}$, then C , D and \bar{C} represent the covariance of noise in the signal part of y , covariance of measuring errors and covariance of observations respectively. If the signal and noise are uncorrelated as generally expected, since y is the result of direct measurement, then the cross covariances are zero i.e.

$$C_{\epsilon s} = 0; \quad C_{s'\epsilon} = 0. \quad (2.2.1-6)$$

hence from (2.2.1-3) we have that;

$$C_{yy} = C_{s's'} + C_{\epsilon\epsilon} \quad \text{or} \quad \bar{C} = C + D. \quad (2.2.1-7)$$

If we further assume no correlation between signal and noise, then we have that,

$$C_{sy} = E\{sz^T\} = E\{s(s' + \epsilon^T)\} = E\{ss'^T\} + E\{s\epsilon^T\} = E\{ss'\}. \quad (2.2.1-8)$$

so that

$$C_{sy} = \text{cov}(s, s'), \dots \dots \dots C_{ys} = \text{cov}(s', s). \quad (2.2.1-9)$$

with C_{sy} and C_{ys} as pure signal covariances. All these covariances are assumed to be known or can be approximated. Now for the vector r in (2.2.1-4) we can write (2.2.1-3) as,

$$\mathbf{AX} + \mathbf{Br} - \mathbf{y} = \mathbf{0}. \quad (2.2.1-10)$$

with $\mathbf{B} = [\mathbf{0} \quad \mathbf{I}]$; Equation (2.2.1-10) has the form of condition equations with parameters (i.e. combined case). We can proceed and apply least squares technique i.e.

$$\mathbf{r}^T \mathbf{P} \mathbf{r} \Rightarrow \text{Minimum}. \quad (2.2.1-11)$$

with the condition in equation (2.2.1-10) where \mathbf{P} is the weight matrix given as \mathbf{Q}^{-1} and \mathbf{Q} given as in equation (2.2.1-5).

The function to be minimized for a least squares solution may be expressed as,

$$\phi = \frac{1}{2} \mathbf{r}^T \mathbf{P} \mathbf{r} - \mathbf{k}^T (\mathbf{AX} + \mathbf{Br} - \mathbf{y}). \quad (2.2.1-12)$$

where \mathbf{k} are Lagrange multipliers. From (2.2.1-12) we have that,

$$\mathbf{A}^T (\mathbf{BP}^{-1} \mathbf{B}^T)^{-1} \mathbf{AX} = \mathbf{A}^T (\mathbf{BP}^{-1} \mathbf{B}^T)^{-1} \mathbf{y}. \quad (2.2.1-13)$$

which gives the solution for \mathbf{X} while the solution for \mathbf{r} is given by *Moritz (1980)* as,

$$\mathbf{r} = \mathbf{P}^{-1} \mathbf{B}^T (\mathbf{BP}^{-1} \mathbf{B}^T)^{-1} (\mathbf{y} - \mathbf{AX}). \quad (2.2.1-14)$$

For a special case where \mathbf{B} -matrix = $[\mathbf{0} \quad \mathbf{I}]$ we readily find that,

$$\mathbf{BP}^{-1} \mathbf{B}^T = \mathbf{BQB}^T = [\mathbf{0} \quad \mathbf{I}] \begin{bmatrix} \mathbf{C}_{ss} & \mathbf{C}_{sy} \\ \mathbf{C}_{ys} & \mathbf{C}_{yy} \end{bmatrix} \begin{bmatrix} \mathbf{0} \\ \mathbf{I} \end{bmatrix} = \mathbf{C}_{yy} = \bar{\mathbf{C}}. \quad (2.2.1-15)$$

hence equation (2.2.1-13) gives the solution for the parameters (\mathbf{X}) as,

$$\mathbf{X} = (\mathbf{A}^T \bar{\mathbf{C}}^{-1} \mathbf{A}) \bar{\mathbf{C}}^{-1} \mathbf{y}. \quad (2.2.1-16)$$

From (2.2.1-14) we can write,

$$\mathbf{r} = \mathbf{QB}^T \bar{\mathbf{C}}^{-1} (\mathbf{y} - \mathbf{AX}). \quad (2.2.1-17)$$

Now using equation (2.2.1-4) we have that,

$$\mathbf{r} = \begin{bmatrix} \mathbf{s} \\ \mathbf{z} \end{bmatrix} = \begin{bmatrix} \mathbf{C}_{ss} & \mathbf{C}_{sy} \\ \mathbf{C}_{ys} & \mathbf{C}_{yy} \end{bmatrix} \begin{bmatrix} \mathbf{0} \\ \mathbf{I} \end{bmatrix} \overline{\mathbf{C}}^{-1} (\mathbf{y} - \mathbf{AX}). \quad (2.2.1-18)$$

so that,

$$\mathbf{s} = \mathbf{C}_{sy} \overline{\mathbf{C}}^{-1} (\mathbf{y} - \mathbf{AX}). \quad (2.2.1-19)$$

which gives the solution for the prediction of the signal(s). The equations (2.2.1-16 and (2.2.1-19) provide determination and prediction of unknown parameters and predicted signals respectively. The sum of predicted signals (s) and the interpolated part (AX) gives the geoid height at interpolation points.

The expression for the accuracy estimates of the parameters in LSC is given as,

$$\mathbf{Cov}_x = \mathbf{E}_{xx} = \left[\mathbf{A}^T \overline{\mathbf{C}}^{-1} \mathbf{A} \right]^{-1}. \quad (2.2.1-20)$$

while the accuracy estimates of signals are evaluated as,

$$\mathbf{Cov}_s = \mathbf{E}_{ss} = \mathbf{C}_{ss} - \mathbf{C}_{sy} \overline{\mathbf{C}}^{-1} \left[\mathbf{I} - \mathbf{A}(\mathbf{A}^T \overline{\mathbf{C}}^{-1} \mathbf{A})^{-1} \mathbf{A}^T \overline{\mathbf{C}}^{-1} \right] \mathbf{C}_{ys}. \quad (2.2.1-21)$$

2.2.2 Geopotential Models

The first harmonic coefficients determined at the beginning of the space age were the zonal terms (*Kozai, 1959,1964*) from optical observations. The first global models up to degree and order 6 were determined by *Guier and Newton (1965)* and *Anderle (1966)*, who used numerical integration and Doppler measurements. *Izsak (1966)* applied analytical methods using optical data only. *Kaula (1966b)* was the first to combine satellite orbit perturbation analysis and gravity measurements.

By 1986, numerous models had been computed, improved from time to time principally by four groups. Each used its own methodology, algorithms and software, but still shared a lot of common data. The groups were;

- The Naval Surface Weapons Centre (under the leadership of Anderle).

- The Smithsonian Astrophysical Observatory (under the leadership of Gaposchkin).
- The Goddard Space Flight Centre [under the impulse of many people (Marsh, Wagner, Kiosko, Lerch, among others)].
- The Groupe de Recherches de Géodésie Spatiale (France) and the Deutsche Geodätisches Forschungs Institut (FRG).

A number of earth models have been computed since the 1960's. The modern models can provide the geoid heights of any points on the earth's surface with an accuracy ranging from 30cm to a few meters (*Rapp 1997*). The more recent models consist of geocentric coordinates of tracking stations, a set of harmonic coefficients and the parameters of the geoid. A good example is the WGS84 reference system that is used for NAVSTAR/GPS navigation. Some of the commonly used recent earth models are: EGM96 and OSU91A. The EGM96 is the result of the cooperation of NASA-GSFC and NIMA. New improved gravity data from regions of the earth which were not available before (e.g. from China, former USSR, South America and Africa) together with satellite altimeter data, airborne gravity data over Greenland and Arctica were incorporated in the EGM96 model.

EGM96 has been used in this work. Using the latest theoretical corrections, research, software algorithms, extensive global satellite altimetry, and gravity data, a new model WGS84 (EGM96) geoid has recently been computed by NIMA and NASA. Its absolute accuracy is estimated as $\pm 25\text{cm}$ over the ocean areas while over the land, the absolute accuracy varies from $\pm 50\text{cm}$ and $\pm 2\text{m}$ (<http://www.nima.mil/GrandG/wgsegm/egm96.html>).

The NIMA/NASA geoid height file consists of a 0.25-degree grid of point values in the tide-free system, using the EGM96 geopotential model to degree and order 360. The WGS84 constants (a , f , GM and ω) have been used to define the geometry and the normal field of reference ellipsoid in the calculation of this geoid height file. The geoid undulation values are computed by applying a correction term that converts range anomaly calculated at a point on the reference ellipsoid to a geoid undulation value. In addition, a correction term of -0.53m is added to the prior result to obtain the geoid undulation with respect to the WGS84 ellipsoid.

The 15-minute geoid height grid is used as an input to a FORTRAN program, INTPT.F. developed for interpolating from the grid, a geoid undulation at any given WGS84 latitude

and longitude. The program F477.F requires both the EGM96 spherical harmonic coefficient file and the correction coefficient file to calculate point geoid undulations by spherical harmonic synthesis (<http://www.nima.mil/GrandG/wgsegm/egm96.html>).

Geopotential models are being used as reference fields for local and regional geoid determination today. However, it should be noted that for the available models, the medium and short wavelength coefficients have large errors and not as reliable as the coefficients of the long wavelength (*Rapp, 1986; Sideris and Schwarz, 1986; Schwarz et al. 1987*). Precise determination of medium and short wavelength signals of the geoid height can be achieved by various strategies. One way of resolving the effects of medium and short wavelengths is truncation of spherical harmonic expansion to a certain low degree and extending the size of the area within which the data is evaluated by the LSC method (*Sideris and Schwarz, 1986*). The other method depends on a tailored geopotential model, which is tailored to the available gravity anomalies in a certain area (*Weber and Zomorrodian, 1988; Torge et al. 1989; Kearsley and Forsberg, 1990*).

2.2.3 Interpolating Polynomial

Interpolating polynomial may be defined simply as a function that can be used to determine certain values where observations have not been done. A function is specified as a set of values at discrete set of argument points. This situation occurs when the function comes from physical process and is only known by measuring the value of the function at various argument points or equivalently, when the data values are the result of previous computation(s) (*Pizer, 1975*). Given $n+1$ distinct (real or complex) points z_0, z_1, \dots, z_n and $n+1$ (real or complex) values $\omega_0, \omega_1, \dots, \omega_n$; there exists a unique polynomial, $p_n(z) \in \mathcal{P}_n$ for which $p_n(z_i) = \omega_i$; $i = 0, 1, \dots, n$. (*Davis, 1975*).

Several interpolating polynomials (linear and surface) exist. The linear polynomials may include Lagrange, Newton divided-difference, Iterated linear, Orthogonal and Remainder theory polynomials among others (*Davis, 1975*). These linear polynomials may also be extended into surface polynomials. The commonly used surface polynomials for DTMs (Digital Terrain Models) generation in a GIS (Geographic Information Systems) environment are; bilinear, biquadratic and bicubic polynomials. These surface polynomials are linear and easy to manipulate. They require lesser computer time and are generally accurate depending on the surface being modelled. The three (1st, 2nd and 3rd order) surface polynomials may be expressed respectively as,

$$N_i = k_0 + k_1 X_i + k_2 Y_i + k_3 X_i Y_i. \quad (2.2.3-1)$$

$$N_i = k_0 + k_1 X_i + k_2 Y_i + k_3 X_i Y_i + k_4 X_i^2 + k_5 Y_i^2 + k_6 X_i^2 Y_i + k_7 X_i Y_i^2 + k_8 X_i^2 Y_i^2. \quad (2.2.3-2)$$

$$N_i = k_0 + k_1 X_i + k_2 Y_i + k_3 X_i Y_i + k_4 X_i^2 + k_5 Y_i^2 + k_6 X_i^2 Y_i + k_7 X_i Y_i^2 + k_8 X_i^2 Y_i^2 + k_9 X_i^3 + k_{10} Y_i^3 + k_{11} X_i^3 Y_i + k_{12} X_i Y_i^3 + k_{13} X_i^3 Y_i^3 + k_{14} X_i^3 Y_i^2 + k_{15} X_i^2 Y_i^3. \quad (2.2.3-3)$$

where,

N_i is geoid height at point i ,

X_i, Y_i are plane coordinates at point i ,

k_0, k_1, \dots, k_{15} are coefficients.

The second order polynomial (2.2.3-2) has been used in this work due to the limitation of data and the fact that the change in gradient of geoid over a small area is generally uniform and gentle.

CHAPTER THREE

HEIGHT SYSTEMS AND GLOBAL POSITIONING SYSTEM

3.1 Height Systems

It had long been recognized that the use of geocentric distances would be desirable to avoid the uncertain factor of the geoid, which is the reference ellipsoid separation. This is however, not convenient because the origin of the earth is not accessible and most if not all earth measuring instruments cannot be oriented to it. Hence its position must be deduced from multiple observations. Thus in practice elevations are generally referred to mean sea level or geoid. Heights provide the third dimension in geodetic positioning. Height can be basically defined as the measure of length along a normal to a datum surface. The datum surface depends on the type of height system. There are various height systems e.g. orthometric heights, geodetic heights, dynamic heights, normal heights, Vignal heights, Helmert's heights, normal orthometric heights, bathymetric heights, barometric heights, etc. In this work, two types of height systems (geodetic and orthometric heights) have been used.

3.1.1 Orthometric Heights

Orthometric height is defined generally as the geometrical distance between the geoid and the point (on the terrain surface), measured along the plumb line at the point. The orthometric height may be represented geometrically as given in Figure 3.1.1.1 and mathematically as given in equation 3.1.1-1.

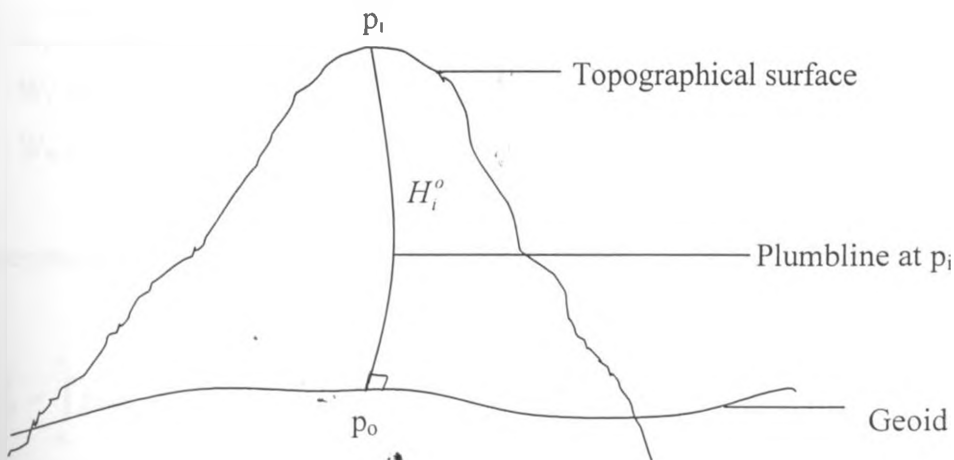


Figure: 3.1.1.1: Orthometric height

$$H_i^o = \int_{p_o}^{p_i} dh' \quad (3.1.1-1)$$

where,

H_i^o is the orthometric height of a point p_i on the topographical surface.

p_o is the projection of p_i on the geoid along the plumb line through p_i .

p_i is a point on the topographical surface.

dh' is the height difference

The integration is along the plumb line and if we substitute for $dh' \cong \delta h$ given as,

$$\delta h = -\frac{\delta W}{g} \quad (3.1.1-2)$$

where δW is the difference in potential for two equipotential surfaces and g is the actual gravity at a point p_i on the topographical surface, then we have that,

$$H_i^o = -\int_{p_o}^{p_i} \frac{dW}{g_i} \quad (3.1.1-3)$$

in which we denote the gravity along the plumb line as g' . But we also have,

$$C_i = -(W_i - W_o) = \int_{p_o}^{p_i} g dn = \int_{p_o}^{p_i} g' dh' = dW \quad (3.1.1-4)$$

where, C_i is the geopotential number at p_i ,

W_i is the potential at terrain point p_i ,

W_o is the potential at the geoid p_o .

The geopotential number difference between two points (p_i and p_j) is practically evaluated as,

$$\Delta C_{ij} = \int_{p_i}^{p_j} g dn \quad (3.1.1-5)$$

where,

ΔC_{ij} is the geopotential number difference between points i and j .

dn is the orthometric height difference.

Using (3.1.1-4) and (3.1.1-5), (3.1.1-3) may be expressed as,

$$H_i^o = \int_{p_o}^{p_i} \frac{dC}{g_i} = \int_{p_o}^{p_i} \frac{g dn}{g_i} \quad (3.1.1-6)$$

Now using the mean gravity (\bar{g}) between the geoid and the terrain point we can write (3.1.1-6) as,

$$H_i^o = \frac{1}{\bar{g}} \int_{p_o}^{p_i} g dn \quad (3.1.1-7)$$

then the orthometric height of a point p_i is obtained from the evaluation of the integral in equation (3.1.1-7), which results to equation 3.1.1-8 below (*Heiskanen and Moritz, 1967*).

$$H_{p_i}^o = \frac{C_i}{g_i} \quad (3.1.1-8)$$

Orthometric height correction is needed to convert measured height differences (from spirit leveling) into differences of orthometric heights. The correction for a levelled line from point i to j can be expressed as,

$$OC_{ij} = \sum_i^j \frac{g - \gamma_o}{\gamma_o} \delta n + \frac{\bar{g}_i - \gamma_o}{\gamma_o} H_i^o - \frac{\bar{g}_j - \gamma_o}{\gamma_o} H_j^o \quad (3.1.1-9)$$

where, g is the actual gravity, γ_o is the normal gravity at latitude 45° ,

\bar{g}_i and \bar{g}_j are the mean values of gravity along the plumb line at point i and j respectively,

δn is the levelled height difference between instrument set – ups.

3.1.2 Geodetic Heights

A geodetic height is defined as the distance of the point above a reference ellipsoid measured along the normal at the point to the ellipsoid. Geodetic heights use reference ellipsoid as the datum. The use of geodetic heights is becoming very crucial in three dimensional positioning in which the geodetic coordinates are expressed as the curvilinear coordinates: - latitude (ϕ), longitude (λ) and ellipsoidal height (h). Geodetic height may be represented geometrically as shown in Figure 3.1.2.1.

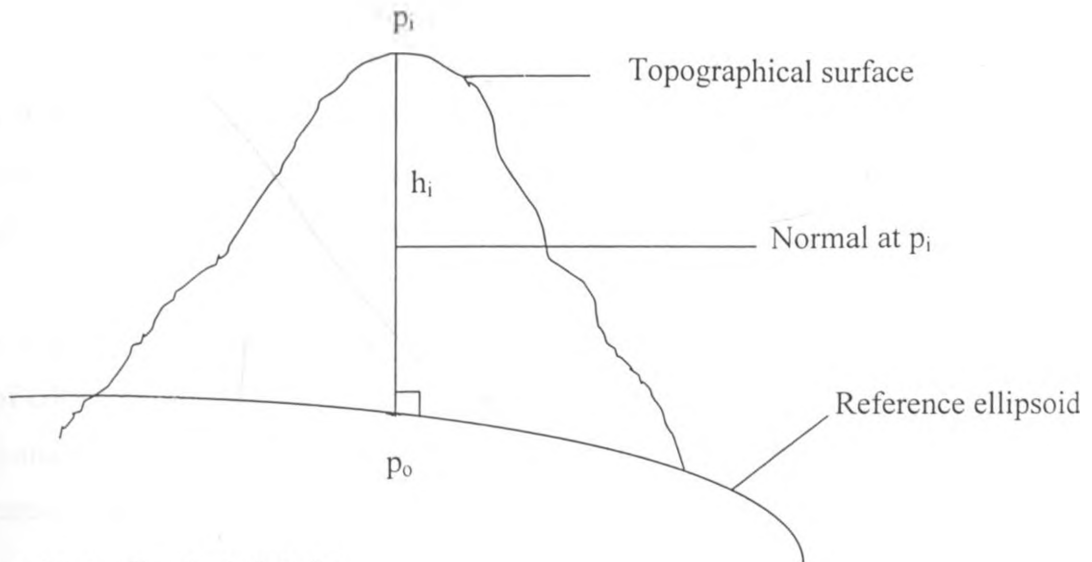


Figure 3.1.2.1: Geodetic height

where,

h_i is the geodetic height of a point p_i on the topographical surface,

p_o is the projection of p_i on the reference ellipsoid along the normal through p_i .

p_i is a point on the topographical surface.

3.2 Global Positioning System

The NAVSTAR-GPS system was developed as a logical improvement on the TRANSIT system. The system however is commonly referred to as GPS. The NAVSTAR-GPS is a system for positioning on or near the surface of the earth in three-dimensional space using satellites. It is also used for precise timing. The NAVSTAR-GPS is an American system initially set up for military navigation and positioning on a programme that was started in 1969 by the Department of Defence. The system was eventually opened up to civilians in mid 1980's. It however became fully operational in July 1995.

The system consists of 24 satellites, which are in near circular orbits at altitudes of 20,200 km above the surface of the earth (e.g. Hofmann-Wellenhof et al., 1992). The GPS system is divided into three "interconnected" segments. These include space, control and user segments. The space segment consists of 24 satellites in six orbits and inclined at an angle of 55° to the equatorial plane. The orbits are organized in such a way that at any instant there are twelve satellites above or below the horizon.

The control segment includes the ground monitor, command and control functions. This segment performs the tracking, orbit determination and time synchronization functions (Hofmann-Wellenhof et al., 1992). It also periodically uplinks the computed ephemerides and time information to the satellites (Mueller, 1991). It consists of a set of five terrestrial points strategically located around the world for monitoring the satellites.

The user segment is perhaps the most commonly seen and used component by civilians. It consists of GPS receivers, calibration assemblies and navigation data-processing functions. The receiver consists of antenna, radio frequency unit and microprocessor, oscillator and power supply, memory and user interface.

3.2.1 GPS Coordinates

The GPS coordinates are divided into two categories. These include the inertial coordinate system and the earth - fixed coordinate system. The former refers to coordinate system fixed in space while the latter may be defined as the coordinate system fixed on or near the earth's surface and rotates with the earth. For the purposes of this research the earth fixed coordinate system is discussed. The earth fixed coordinate system may further be divided into two categories; Cartesian and geodetic (ellipsoidal) coordinates as shown in Figure 3.2.1.1 below.

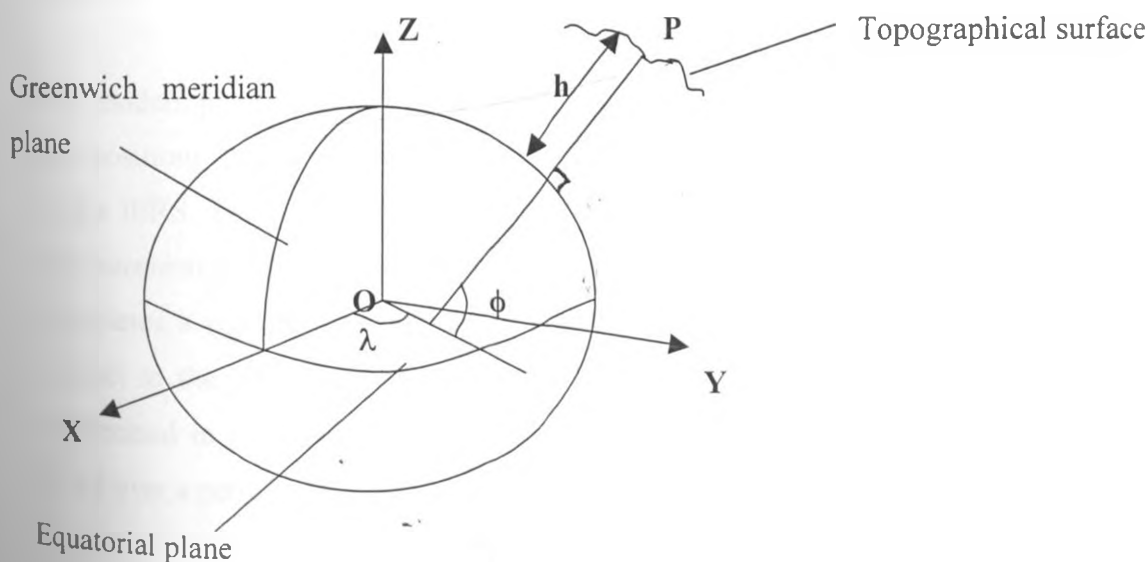


Figure 3.2.1.1: Cartesian and geodetic coordinates

where,

X, Y and **Z** are the Cartesian coordinates,

ϕ , λ and **h** are the geodetic coordinates,

P is a point on the topographical surface and **O** is the centre of mass of the earth.

The GPS satellite coordinates are defined on an ellipsoid of reference called the World Geodetic System 1984 (WGS84). This system is global and geocentric (has origin at the centre of mass of the Earth). The three dimensional position of a point on the surface of the earth is represented by a triplet of coordinates that refer to a particular coordinate system. For the coordinates to be meaningful, the system must be well defined, that is the origin of the system (0, 0, 0) and the coordinate axes must be fixed with respect to the solid earth (*Langley, 1992*).

The struggle to tie different regional datums together for military and other purposes and the advent of satellite-based positioning system asserted the need for a global geodetic reference system. The development of WGS84 may be traced to the Defence Mapping Agency of the United States of America. It was obtained by modifying the Naval Surface Warfare Centre by; lowering the origin of NSWC9Z-2 by 4.5m, rotating the NSWC9Z-2 reference meridian westwards by 0.814 seconds of arc to zero meridian as defined by BIH, and changing scale by 0.6×10^{-6} .

The modern practice locates the origin of the cartesian coordinates at the earth's centre of mass and positions the Z-axis parallel to the CTP as defined by the BIH. The BIH was the forerunner of the IERS. The X- and Y-axes are orthogonal to the Z-axis, with the X-axis passing through the intersection of the zero (reference meridian) and the plane of CTP equator, the Y-axis completes a right-handed coordinate system. The rotation axis actually moves slightly with respect to the solid earth as a result of polar motion, so an average pole position must be determined in order to fix the Z-axis. This determination is time dependent and is done by IERS over a period of 5 years.

The geodetic coordinates are the geodetic; - latitude, longitude and height. The geodetic latitude (ϕ) may be defined as the angle measured in the meridian plane through a point between the equatorial (X, Y) plane of the ellipsoid and line perpendicular or normal to the

surface of a reference ellipsoid at the point. The geodetic longitude (λ) is the angle measured in the equatorial plane between the zero meridian (defined by the X-axis) and the meridian plane through a point while the geodetic height (h) is the distance between a point on the topography and the ellipsoidal surface measured along the ellipsoidal normal, positive in the direction of the zenith.

3.2.2 Accuracy of GPS Surveying

The main accuracy factors (determinants) in GPS surveying are: the satellite configuration, the accuracy of the ephemerides, receiver analysis software and mode of determination. The satellite configuration determines the accuracy from the area occupied by at least four satellites necessary for positioning. A measure of satellite geometry with respect to the observing station is referred to as the Geometric Dilution of Precision (GDOP). Another related factor is the Position Dilution of Precision (PDOP). Therefore it can be deduced that for higher accuracies to be achieved at least four satellites should occupy 'optimum' area in the sky. The satellites should also be distributed in such a way as to form well conditioned triangles and GDOP should be as low as possible. Both GDOP and PDOP are evaluated from the cofactor matrix of the observations given as,

$$Q_{xx} = \begin{bmatrix} q_{xx} & q_{xy} & q_{xz} & q_{xt} \\ q_{yx} & q_{yy} & q_{yz} & q_{yt} \\ q_{zx} & q_{zy} & q_{zz} & q_{zt} \\ q_{tx} & q_{ty} & q_{tz} & q_{tt} \end{bmatrix} \quad (3.2.2-1)$$

from which we obtain GDOP and PDOP as,

$$GDOP = \sqrt{q_{xx} + q_{yy} + q_{zz} + q_{tt}} \quad (3.2.2-2)$$

$$PDOP = \sqrt{q_{xx} + q_{yy} + q_{zz}} \quad (3.2.2-3)$$

In GPS positioning, GPS satellites play a role of reference points in the sky. Thus accuracy of satellite ephemerides is essential for quality control of GPS surveys. The accuracy of the broadcast ephemeris is about $\pm 10\text{m}$ while that of precise ephemeris is $\pm 0.1\text{m}$. The receiver

analysis software hints to the ability to handle varied information relayed via the electromagnetic waves received at the receiver station.

The mode of positioning is also a key factor in the accuracy of GPS surveying. Absolute position accuracies of $\pm 10\text{m}$ in the precise positioning service and $\pm 50\text{m}$ in the standard positioning service. Much higher accuracies can be obtained if GPS is used in the differential mode, determining basically the relative position of a GPS receiver with respect to another at known station (reference station). Accuracies better than one part per million (ppm) in relative positions can be achieved in this mode. Differential position errors of up to 1ppm are resulting from reference station errors of $\pm 10\text{m}$ (Santere, 1989). Differential positioning is the method for the determination of GPS coordinates used in this study.

There are two other intentionally induced errors that affect the accuracy of GPS surveying and any other uses. These include and not limited to selective availability and anti-spoofing. GPS being a military system is prone to situational manipulation by the owners, United States in moments of war. Selective availability may be done via: dithering the satellite clock (δ -process) and the manipulation of ephemeris by truncating orbital information in the navigation message (ϵ -process). Antispoofing on the other hand is a designed feature, which enables the system to “turn off” the p-code through encrypted W-code, resulting in Y-code. Selective availability may be a problem of the past due to the decision by the (US) government (in May, 2000) to stop any further degradation of GPS accuracy.

The above factors are however not complete, there are other factors such as: the orbital determination strategy and GPS observation system itself. The orbital determination strategy includes length of satellite arc and the sophistication of orbital perturbation modules. Factors related to the GPS observation system includes: measurement, modelling, ambiguity resolution and accounting for biases. Other sources of errors in GPS surveying may include signal multi-path effect, ionospheric and atmospheric delays, receiver clock errors, satellite visibility, and receiver noise and phase ambiguity. The delay in the ionosphere can be minimized by utilizing the two waves, L_1 and L_2 . The error due to the multi-path can be reduced by carefully selecting the site for receiver setting (Leick, 1990 and Resch, 1984).

CHAPTER FOUR

LOCAL COORDINATE SYSTEM

4.1 Definitions

A local coordinate system is defined as a two-dimensional map coordinate system based on a selected map projection. The main aim of a local coordinate system is to enable the plotting of base maps of a country, designation of horizontal control network(s), cadastral surveying, engineering surveying, mining surveying and hydrographic surveying.

A map is a plane representation of a curved surface of the ellipsoid (or sphere) on which positions of discrete points are defined. The construction of a map will therefore require the transformation of the ellipsoidal coordinates into plane coordinates. The basic problem of map projection is therefore how to represent the curved surface of the ellipsoid onto a plane.

It should be noted without any confusion that there are varied coordinate and projection systems. The choice of a map coordinate system or projection system depends mainly on the purpose of the map, geographical location and size of the mapping area. Other minor factors may be class of projection by Young's rule and choice by tradition.

For the establishment of a local coordinate system, a local geodetic datum needs to be determined so that the reference ellipsoid conforms as closely as possible to the geoid over the area or country or region to be mapped. This therefore means that grade measurements have to be taken over the defined area for orientation of such a local reference ellipsoid. Hence, the centre of a local reference ellipsoid does not coincide with the centre of the earth in most cases due to limitation of data for the whole earth. The axes are however made parallel by the use of Laplace azimuth equation as given below.

$$A - \alpha = (\Lambda - \lambda) \sin \phi + (\xi \sin \alpha - \eta \cos \alpha) \cot Z_G \quad (4.1-1)$$

Where,

A is astronomic azimuth,

α is geodetic azimuth,

Z_G is geodetic zenith angle,

Λ is astronomic longitude.

The above equation gives the relationship between the astronomic and geodetic azimuths as a function of the deflection of the vertical. In most first order triangulation, $Z_G = 90^\circ$ hence the last term in (4.1-1) is negligible. The expression (4.1-1) therefore becomes,

$$A - \alpha = (\Lambda - \lambda) \sin \phi = \eta \tan \phi. \quad (4.1-2)$$

4.2 Arc Datum 1960

The Arc Datum 1960 is one of the current local reference systems used in this country (Kenya). It is therefore necessary to briefly elaborate on its development and subsequent establishment.

The Kenyan horizontal datum is based on the modified Clarke 1880 (for Universal Transverse Mercator Coordinates) biaxial ellipsoid with its origin in South Africa at Buffelsfontein ($\phi = -33^\circ 59' 32.''000$, $\lambda = 25^\circ 30' 44.''622$) near port Elizabeth (*Rens and Merry, 1990*). Only the azimuth is defined for this datum, the geoidal deviation parameters at the point are by implication zero (*Rens and Merry, 1990*). The parameters are actually not zero as was later observed (*Merry, 1978*). The scale of the datum was provided by a baseline measured along the 30th meridian and thus the name Arc Datum. *Gill (1896)* was aware of these deficiencies when fitting the datum and recommended modification for further geodetic extension.

The position of the geoid relative to the reference ellipsoid is given normally by the geoidal deviation parameters; N (geoidal undulation), ξ and η components (in the north-south and east-west directions respectively) of the deviation of the vertical. In Kenya the average undulation N is about 290m and the deflection of the vertical is around 14" (*Mwakuchengwa, 1994*).

Work on primary triangulation control points was first conducted in Kenya in 1902. Further field observations for primary control points were carried out during the period 1950 – 1960 (*Rogers, 1982*). In 1950 the Directorate of Overseas Surveys of the United Kingdom in co-operation with the Government Survey Departments of Kenya, Uganda and Tanzania undertook to establish a comprehensive horizontal control network within the three East African countries (*Aseno et al. 1994*). Within Kenya, this was scaled by three baselines: Isiolo base (21km), Kisumu base (16km) and Malindi base (13km). The bases were measured and astronomic observations made at suitable stations in each base. Within the network in general, Laplace stations were observed for azimuth checks and determination of the geoid – spheroid separation.

This network was adjusted as part of comprehensive adjustment for Eastern and Central African countries, based on the 30th meridian (*Rainsford, 1951*). This adjustment extended from Southern Rhodesia (current Zimbabwe) in the south to Uganda in the north with positions in the former kept fixed. The results from this adjustment were labeled new (1950) Arc Datum. Later on in 1960 the network was readjusted holding the 30th Arc meridian stations fixed. By this time a gap between Uganda and Sudan networks had been surveyed. The results from this adjustment were termed the new (1960) Arc Datum. The values were computed on the UTM projection based on the Clarke 1880 modified reference ellipsoid.

4.3 Universal Transverse Mercator Coordinate System

This is a grid coordinate system introduced for North Atlantic Treaty Organization (NATO) maps and surveys of the early 1950's. It is designed to cover the whole world between latitudes 80° S and 84° N with uniform system of maps. The following are the major specifications for the coordinate system:

- (i) Conformality (to minimize directional errors hence maintain shapes).
- (ii) Continuity over sizeable areas coupled with minimum number of zones.
- (iii) Scale errors not to exceed a specified tolerance (1/2500).
- (iv) Unique and identifiable referencing in a plane rectangular coordinate system for all zones.
- (v) Transformation formulae (zone to zone) to be uniform throughout assuming the same reference ellipsoid.
- (vi) Meridian convergence not to exceed 5°.

4.3.1 UTM Grid Coordinates

On the basis of criteria in (4.3) a modification of the Transverse Mercator projection was developed as the UTM grid coordinate system for worldwide application. It has the following features (characteristics):

1. The world is divided into 60 zones, each extending through 6° longitude. The zone numbering starts with zone one (1) from 180° W to 174° W with a central meridian of 177° and the numbering continues eastwards. The central meridian is given by $\lambda_{cm} = -6^\circ (30 - N) - 3^\circ$, or alternatively the zone number, N, is given as $N = 30 + (\lambda_{cm} + 3^\circ) / 6$. In this study the zone is 37 with central meridian being 39°E.

2. A scale distortion or grid scale constant of $K_0 = 0.9996$ along the central meridian of each zone is used so as to limit the scale error to 1/2500.
3. A scale is to be used between latitude 84° N and 80° S with the polar regions using the Universal Polar Stereographic (UPS) projection system (which complements the UTM, but independent of it) with overlaps along the boundaries of the two systems.
4. A plane rectangular coordinate system is superimposed on each zone assigning the following values:
 - East of central meridian = 500,000m (as false Easting).
 - Equator is assigned 0m for points north of the equator while a value of 10,000,000m is assigned to the equator for points south of the equator.
5. Zone overlap is about 80 km at each grid junction or 40 km on either side of the zone boundary.
6. Each system is to be based as far as possible on the same figure of the earth. Clarke 1866 ellipsoid was proposed but it is not used by all countries of the world. The commonly used figures of the earth are Bessel 1841, Clarke 1880 (Africa), Everest (Europe) and the International ellipsoids.

4.3.2 UTM Mapping Equations

In the UTM, a secant cylinder is used. It intersects the sphere (ellipsoid) at about 180km east and west of the central meridian, so that the scale factor at the central meridian is $K_0 = 0.9996$ (an assigned value). The choice of this value was made so as to limit the scale error to 0.0004 or 1/2500 within the 6° -longitude width zone. The following are therefore the planimetric mapping equations for UTM incorporating the secant cylinder and maintaining the scale factor of 0.9996 on the central meridian (*e.g. Maling, 1973*).

$$N = K_0 \left\{ S\phi + \frac{v}{2} (\Delta\lambda \cos\phi)^2 \tan\phi + \frac{v}{24} (\Delta\lambda \cos\phi)^4 \tan\phi (5 - \tan^2\phi) + \dots \right\}. \quad (4.3.2-1)$$

$$E = K_0 \left\{ v\Delta\lambda \cos\phi + \frac{v}{6} (\Delta\lambda \cos\phi)^3 \left(\frac{v}{\rho} - \tan^2\phi \right) + \frac{v}{120} (\Delta\lambda \cos\phi)^5 (5 - 18 \tan^2\phi + \tan^4\phi) + \dots \right\}.$$

(4.3.2 - 2)

The scale factor K_p , at any point P on the map may be given as,

$$K_p = K_0 \left(1 + \frac{E_p^2}{2\rho\nu} \right) \quad (4.3.2 - 3)$$

where,

E_p is the easting value at point P,

ρ is the radius of curvature in the prime vertical direction,

ν is the radius of curvature in the meridian direction.

For a line between two points A and B, the scale factor K_{AB} , to be used is the mean of the scale factors A and B i.e.

$$K_{AB} = \frac{1}{2} (K_A + K_B) \quad (4.3.2 - 4)$$

or

$$K_{AB} = K_0 \left(1 + \frac{E_A^2 + E_A E_B + E_B^2}{6\nu_m \rho_m} \right) \quad (4.3.2 - 5)$$

where,

K_A is the scale factor at point A,

K_B is the scale factor at point B,

E_A is the easting value at point A,

E_B is the easting value at point B,

ν_m is the mean radius of curvature in the prime vertical direction,

ρ_m is the mean radius of curvature in the meridian direction.

4.3.3 Grid to Geodetic Conversion and vice versa

The UTM grid coordinates may be transformed to geodetic coordinates via two methods: iterative and conventional UTM tables (interpolation). The former method involves initial approximation of ϕ and λ followed by a number of iterative processes until the desired results are obtained. The latter involves interpolating the values of ϕ and λ from the conventional UTM tables. These tables have been prepared to facilitate the Gauss–Kruger projection equations. They enable the conversion from geodetic to grid coordinates and vice-versa, and are very handy and practical, particularly where there is no access to a mainframe (or personal) computer.

Iterative procedure may be as summarized below,

- (i) The approximate ϕ and $\Delta\lambda$ can be obtained from

$$\phi^{(i)} = \frac{N'}{R} \quad \text{and} \quad \Delta\lambda^{(i)} = \frac{E'}{v^{(i)} \cos \phi^{(i)}} \quad (4.3.3 - 1)$$

where,

$N' = (10,000,000 - N)$ m in the Southern Hemisphere

$= N$ (m) in the northern hemisphere,

$E' = (E - 500,000)$ m east of central meridian

$= (500,000 - E)$ m west of central meridian,

(4.3.3 - 2)

R is the mean radius of curvature of an equivalent sphere given as,

$$R = \frac{2a + b}{3} \quad (4.3.3 - 3)$$

where,

a is the length of the semi-major axis of the reference ellipsoid,

b is the length of the semi-minor axis of the reference ellipsoid.

- (ii) Using the above approximation for ϕ and $\Delta\lambda$, values for northings and eastings, $N^{(i)}$, $E^{(i)}$ are obtained. These may differ from the given values by amounts, $\delta N = N - N^{(i)}$ and $\delta E = E - E^{(i)}$.

- (iii) The latitudes, $\phi^{(1)}$ and longitude difference $\Delta\lambda^{(1)}$ are now corrected by amounts,

$$\delta\phi = \frac{\delta N}{\rho^{(1)}} \quad \text{and} \quad \delta\Delta\lambda = \frac{\delta E}{v^{(1)} \cos \phi^{(1)}} \quad (4.3.3 - 4)$$

to give better estimates.

- (iv) The new estimates for ϕ and $\Delta\lambda$ are used in stage (ii) above to get differences, δN and δE between computed coordinates and given coordinates.
- (v) The iterative processes of stages (iii) and (iv) are repeated until there is no difference in the UTM coordinates i.e. $\delta N = 0$ and $\delta E = 0$. Now the i^{th} values of $\phi^{(i)}$ and $39 \pm \Delta\lambda^{(i)}$ in stage (iii) will be the converted geodetic coordinates for the given grid coordinates.

The conversion of geodetic coordinates into grid coordinates may be done via two methods. The first method involves the use of equations 4.3.2-1 and 4.3.2-2 for Northing and Easting respectively. The second method is achieved by the use of conventional UTM tables.

CHAPTER FIVE

COORDINATE TRANSFORMATIONS

5.1 Introduction

The existing geodetic control networks in various parts of the world are usually rotated to regionally defined datums. The reference ellipsoids of some of those datums happen to be directly compatible with the geocentric WGS84 ellipsoid whereas sizeable differences occur for other datum having non-geocentric reference ellipsoids e.g. the Arc-Datum 1960. This therefore necessitates the determination of transformation parameters between WGS84 and other local systems to enable the use of GPS for local surveys.

The effect of a transformation varies from simple changes of location and direction, to a uniform change in scale and finally to change in shape and size of degree of linearity. There is therefore a whole family of transformations, some of which are applicable to two-dimensional space and others for use in three-dimensional space (system). The former refers to transformation between plane coordinates e.g. (X, Y) and (x, y), while the latter refers to the transformation between triplet sets of coordinates e.g. (X, Y, Z) and (x, y, z).

The common models used for transformation are: Bursa-Wolf, Molodensky, Differential Projective and Molodenskii Badekas. This study concentrates on Bursa-Wolf and Molodensky models for three-dimensional transformation.

5.2 Transformation between Geodetic and Cartesian Coordinates

Geodetic coordinates can be converted / transformed to cartesian coordinates (X, Y, Z) via the equations below (e.g. Heiskanen and Moritz, 1967).

$$\begin{aligned} X &= (v + h) \cos\phi \cos\lambda, \\ Y &= (v + h) \cos\phi \sin\lambda, \\ Z &= [v(1 - e^2) + h] \sin\phi. \end{aligned} \tag{5.2-1}$$

the reverse process of determining (ϕ, λ, h) from (X, Y, Z) may be as follows.

$$\lambda = \tan^{-1}\left(\frac{Y}{X}\right). \tag{5.2-2}$$

The geodetic latitude may be obtained by two methods; iterative and non iterative given in eqns (5.2-3) and (5.2-4) respectively (Bowring, 1978).

$$\phi = \tan^{-1} \left[\frac{Z + Ze^2 v \sin \phi}{(X^2 + Y^2)^{\frac{1}{2}}} \right] \quad (5.2-3)$$

$$\phi = \tan^{-1} \left[\frac{Z + e'^2 . b . \sin^3 \theta}{P - e^2 . a . \cos^3 \theta} \right] \quad (5.2-4)$$

while geodetic height is given as,

$$h = \frac{(X^2 + Y^2)^{\frac{1}{2}}}{\cos \phi} - v. \quad (5.2-5)$$

where,

(X, Y, Z) are cartesian coordinates,

(ϕ, λ, h) are geodetic coordinates,

e is the first eccentricity,

e' is the second eccentricity,

v is the radius in the prime vertical,

a is the length of the semi-major axis of the reference ellipsoid,

b is the length of the semi minor axis of the reference ellipsoid.

and also

$$P = (X^2 + Y^2)^{\frac{1}{2}}. \quad (5.2-6)$$

$$\theta = \tan^{-1} \left(\frac{Za}{Pb} \right). \quad (5.2-7)$$

5.3 Datum Transformation

Datum may be defined as any conventional framework into which observations are referred in a given locality or globally. A geodetic datum therefore refers to a specifically oriented reference ellipsoid upon which geodetic observations are carried out or based. Eight parameters are required to define a geodetic datum: two to specify the dimensions of the ellipsoid, three to specify the location of its centre with respect to the centre of the earth and three to specify the orientation of the ellipsoid.

Datum transformation then refers to the determination of parameters that relate two reference systems. In the specific case of GPS positioning, the interest is always in the transformation of coordinates of points between WGS84 system and other systems. Usually in such case (s), the WGS84 system is considered as the reference with respect to which the transformation of the other system would be taken.

5.3.1 Three Dimensional Transformation

A similarity three dimensional coordinate transformation between X, Y, Z and x, y, z coordinate frames is the seven parameter transformation which allows for three rotations, three translations and one uniform scale change. The seven parameters are required to rigorously transform coordinates from one three dimensional cartesian system with a different origin, scale and spatial orientation. The expression for the three dimensional transformation is given as;

$$\begin{bmatrix} X_i \\ Y_i \\ Z_i \end{bmatrix} = qRc \begin{bmatrix} x_i \\ y_i \\ z_i \end{bmatrix} + \begin{bmatrix} X_0 \\ Y_0 \\ Z_0 \end{bmatrix} \quad (5.3.1-1)$$

The reverse transformation being

$$\begin{bmatrix} x_i \\ y_i \\ z_i \end{bmatrix} = \frac{1}{q} Rc' \begin{bmatrix} X_i - X_0 \\ Y_i - Y_0 \\ Z_i - Z_0 \end{bmatrix} \quad (5.3.1-2)$$

where,

q is a uniform scale change,

R_c is a 3 x 3 orthogonal cardanian rotation matrix,

X_0, Y_0, Z_0 are the translation components,

X_i, Y_i, Z_i are the WGS84 coordinates,

x_i, y_i, z_i are the Arc Datum 1960 coordinates.

If the coordinates of three stations are known exactly in both systems then the values of the seven parameters may be calculated exactly. In geodesy this is not the case as the station coordinates are the result of an adjustment of observations and thus more stations are required and the parameters are found by a least squares solution (*Allman and Veenstra, 1982*). Hence the use of seven stations in this work. In this study the Gauss Markov model has been used to obtain the desired solution (s).

5.3.1.1 Rotation Matrices

In coordinate transformations we generally have to rotate one cartesian coordinate frame into another, including scaling and translating the frame being transformed into the other. For such orthogonal frames, one frame is rotated into the other through anti-clockwise angular rotations θ_1, θ_2 and θ_3 about the first, second and the third axes respectively. There are therefore three rotations given as,

$$R_1(\theta_1) = \begin{bmatrix} 1 & 0 & 0 \\ 0 & \cos \theta_1 & \sin \theta_1 \\ 0 & -\sin \theta_1 & \cos \theta_1 \end{bmatrix}. \quad (5.3.1.1-1)$$

$$R_2(\theta_2) = \begin{bmatrix} \cos \theta_2 & 0 & -\sin \theta_2 \\ 0 & 1 & 0 \\ \sin \theta_2 & 0 & \cos \theta_2 \end{bmatrix}. \quad (5.3.1.1-2)$$

$$R_3(\theta_3) = \begin{bmatrix} \cos \theta_3 & \sin \theta_3 & 0 \\ -\sin \theta_3 & \cos \theta_3 & 0 \\ 0 & 0 & 1 \end{bmatrix}. \quad (5.3.1.1-3)$$

$R_1(\theta_1)$ denotes the rotation on the base vector of the first axis through an angle θ_1 . $R_2(\theta_2)$ and $R_3(\theta_3)$ denote similar rotations through angles θ_2 and θ_3 about second and third base vectors respectively.

A cardanian rotation matrix has been used in this research. In this approach all the three rotations about the base vectors are taken in the order of first, second and third base vectors. The resultant rotation matrix is given as.

$$R_c(\theta_1, \theta_2, \theta_3) = R_3(\theta_3) R_2(\theta_2) R_1(\theta_1). \quad (5.3.1.1-4)$$

Therefore expanding (5.3.1.1-4) we have that,

$$R_c(\theta_1, \theta_2, \theta_3) = \begin{bmatrix} \cos \theta_3 \cos \theta_2 & \cos \theta_3 \sin \theta_2 \sin \theta_1 + \sin \theta_3 \cos \theta_1 & -\cos \theta_3 \sin \theta_2 \cos \theta_1 + \sin \theta_3 \sin \theta_1 \\ -\sin \theta_3 \cos \theta_2 & -\sin \theta_3 \sin \theta_2 \sin \theta_1 + \cos \theta_3 \cos \theta_1 & \sin \theta_3 \sin \theta_2 \cos \theta_1 + \cos \theta_3 \sin \theta_1 \\ \sin \theta_2 & -\cos \theta_2 \sin \theta_1 & \cos \theta_2 \cos \theta_1 \end{bmatrix}.$$

(5.3.1.1-5)

In the special case that the rotation angles are very small then (5.3.1.1-5) is simplified as.

$$R_c(\theta_1, \theta_2, \theta_3) = \begin{bmatrix} 1 & \theta_3 & -\theta_2 \\ -\theta_3 & 1 & \theta_1 \\ \theta_2 & -\theta_1 & 1 \end{bmatrix}. \quad (5.3.1.1-6)$$

where,

θ_1 , θ_2 and θ_3 are the rotation angles about x-, y- and z- axes respectively.

5.3.1.2 Bursa -Wolf Model

The Bursa - Wolf model is given by (5.3.1-1). Expanding (5.3.1-1) and incorporating (5.3.1-6) we obtain (5.3.1.2-1).

$$\begin{bmatrix} X_i \\ Y_i \\ Z_i \end{bmatrix} = q \begin{bmatrix} 1 & \theta_3 & -\theta_2 \\ -\theta_3 & 1 & \theta_1 \\ \theta_2 & -\theta_1 & 1 \end{bmatrix} \begin{bmatrix} x_i \\ y_i \\ z_i \end{bmatrix} + \begin{bmatrix} X_o \\ Y_o \\ Z_o \end{bmatrix} \quad (5.3.1.2-1)$$

The above equations are non-linear. For a solution with least squares, we must then linearise the equations. Taylor series linearisation is used and the linearisation is performed about the approximate values: X_o^1 , Y_o^1 , Z_o^1 , q^1 , θ_1^1 , θ_2^1 and θ_3^1 . Usually the approximate values for scale and the angles of rotation are taken as $q^1 = 1$ and $\theta_1^1 = \theta_2^1 = \theta_3^1 = 0$. This is because the rotation angles are usually very small while the scale only deviates slightly from unit (1). The approximate values for the shifts (X_o^1 , Y_o^1 , Z_o^1) are obtained from the cartesian coordinates on the two systems (WGS84 and Arc-Datum 1960). The linearised Bursa -Wolf model is given as,

$$\begin{bmatrix} X'_i \\ Y'_i \\ Z'_i \end{bmatrix} = \begin{bmatrix} 1 & 0 & 0 & x_i & 0 & -z_i & y_i \\ 0 & 1 & 0 & y_i & z_i & 0 & -x_i \\ 0 & 0 & 1 & z_i & -y_i & x_i & 0 \end{bmatrix} \begin{bmatrix} \Delta X_o \\ \Delta Y_o \\ \Delta Z_o \\ \Delta q \\ \Delta \theta_1 \\ \Delta \theta_2 \\ \Delta \theta_3 \end{bmatrix} + \begin{bmatrix} V_{X_i} \\ V_{Y_i} \\ V_{Z_i} \end{bmatrix} \quad (5.3.1.2-2)$$

5.3.1.3 Molodensky Model

In this approach the rotation parameters are assumed to be zero or of such small magnitudes that they are insignificant. The scale factor is assumed to be unity. Hence only the translation parameters are considered. Equations for this model are given as,

$$\begin{aligned}
(\rho + h)d\phi &= -X_0 \sin \phi \cos \phi - Y_0 \sin \lambda \cos \phi + Z_0 \cos \phi + \frac{e^2 \sin \phi \cos \phi}{(1 - e^2 \sin^2 \phi)^{\frac{1}{2}}} da \\
&+ \sin \phi \cos \phi (2\nu + e'^2 \rho \sin^2 \phi)(1 - f)df \\
(\nu + h)\cos \phi d\lambda &= -X_0 \sin \lambda + Y_0 \cos \lambda \\
dh &= X_0 \cos \phi \cos \lambda + Y_0 \cos \phi \sin \lambda + Z_0 \sin \phi - (1 - e^2 \sin^2 \phi)^{\frac{1}{2}} da + \frac{a(1 - f)\sin^2 \phi}{(1 - e^2 \sin^2 \phi)^{\frac{1}{2}}} df
\end{aligned}
\tag{5.3.1.3-1}$$

where,

$d\phi$, $d\lambda$ and dh are differences in geodetic coordinates between the two datums,
 da and df are the differences between the parameters of the reference ellipsoids used in
the two datums,
 X_0 , Y_0 and Z_0 are the shift parameters.

5.4 Estimation Model

To solve for the transformation parameters an adjustment approach for parameter estimation has been adopted on a simple linear model of C.F. Gauss (1777-1855) and A.A. Markov (1856-1922). This model is commonly referred to as the Gauss Markov Model (GMM). The simple GMM is normally expressed as,

$$\mathbf{y} = \mathbf{Ax} + \mathbf{V}_y. \tag{5.4-1}$$

From which we obtain that,

$$\mathbf{D}(\mathbf{y}) = \sigma_0^2 \mathbf{W}^{-1} \tag{5.4-2}$$

and

$$E(\mathbf{V}_y) = 0 \tag{5.4 -2a}$$

where,

- \mathbf{y} is an $n \times 1$ vector of observations,
- \mathbf{A} is an $n \times u$ full rank matrix of design coefficients,
- \mathbf{x} is an $n \times 1$ vector of unknown parameters,

W is an $n \times n$ positive definite weight matrix of the observational vector y ,

V_y is an $n \times 1$ vector of observation residuals,

n is the number of equations,

σ_0^2 is the apriori variance of unit weight,

u is the number of unknown parameters.

The expression for the solution of the unknown parameters (\hat{x}) is given as,

$$\hat{x} = (A^T W A)^{-1} A^T W y. \quad (5.4-3)$$

5.5 Accuracy Estimation

Even though there are many measures of accuracy estimation of evaluated parameters in geodetic networks, standard errors have been used for analysis in this study for convenience.

The standard errors of the computed parameters can be obtained by taking the square root of the individual diagonal elements in the dispersion matrix. It should be noted that, this is only true if the correlation is assumed to be insignificant ($\text{corr}=0$). The dispersion matrix is given as

$$D(\hat{x}) = \hat{\sigma}_0^2 (A^T W A)^{-1}. \quad (5.5-1)$$

where,

$D(\hat{x})$ is the dispersion matrix for the estimated parameters,

$\hat{\sigma}_0^2$ is the a posteriori variance of unit weight.

also

$$\hat{\sigma}_0^2 = \frac{V_y^T W V_y}{n-u}. \quad (5.5-2)$$

where,

V_y is the vector of observational errors given as,

$$V_y = y - A\hat{x}. \quad (5.5-3)$$

CHAPTER SIX

TEST DATA AND COMPUTATIONS

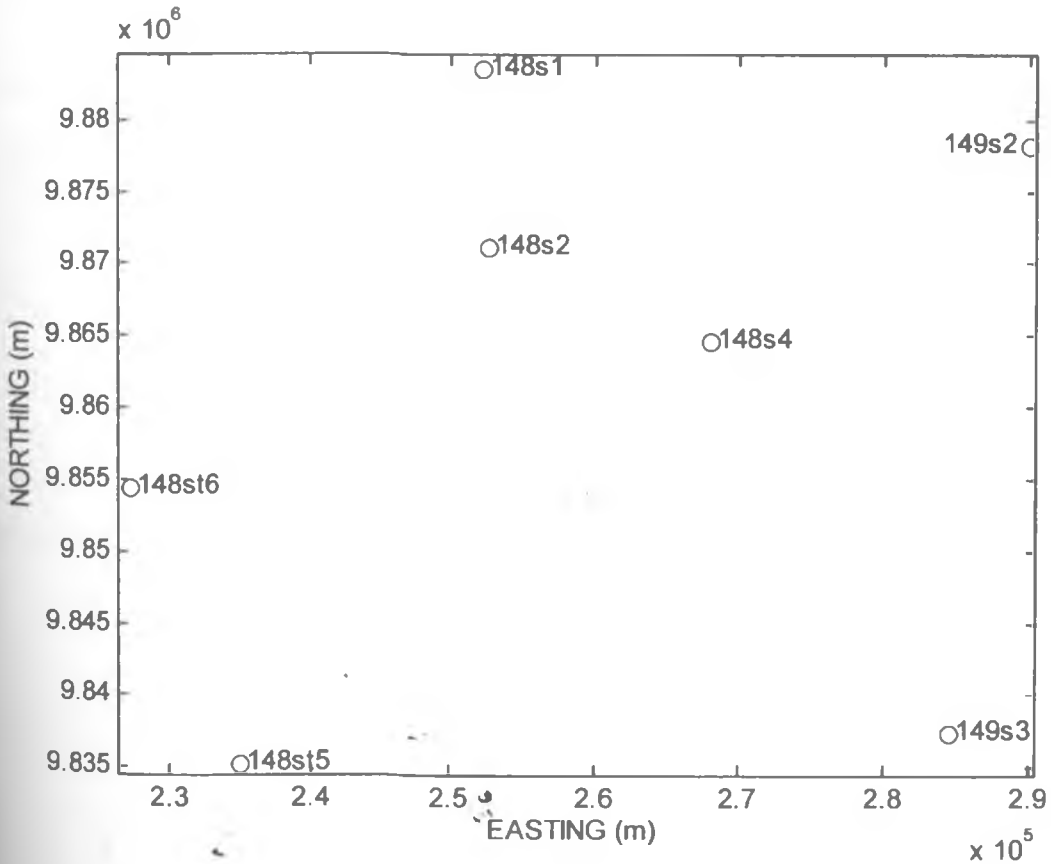
6.1 Triangulation Stations

The description of the triangulation points used for the determination of the transformation parameters are given in Table 6.1.1 and spatial distribution in Figure 6.1.1.

Table 6.1.1: Description of the triangulation points

| Station name (pillar) | Station number | Location |
|-----------------------|----------------|------------|
| Githingire | 148s1 | Kiambu |
| Ndaru | 149s2 | Thika |
| Lukenya | 149s3 | Nairobi |
| Olepelos | 148st5 | Maasailand |
| - | 148st6 | Maasailand |
| Kanunga | 148s2 | Kiambu |
| Marulais | 148s4 | Nairobi |

Figure 6.1.1: Spatial distribution of the triangulation points



6.2 WGS84 and Arc-Datum 1960 Coordinates

Geodetic GPS receivers (Leica CH - 9435) were used for the observations to determine WGS84 coordinates. Post processing was done by Leica ski-pro software. KISM was used as a reference point and the accuracies of its coordinates assumed to be zero. KISM is tied to MALI (at Malindi in Kenya) which is an International Terrestrial Reference Frame (ITRF) point. The horizontal coordinates (geodetic; latitudes and longitudes) were obtained at accuracies between 1mm to 1cm while the vertical coordinates (geodetic heights) were determined to accuracies ranging between 1cm to 8cm.

The WGS84 ellipsoidal curvilinear coordinates are given in Table 6.2.1 while the computed WGS84 ellipsoidal cartesian coordinates are given in Table 6.2.2. The plane UTM coordinates on Arc-Datum 1960 and orthometric heights are given in Table 6.2.3 while the computed geodetic coordinates on the local system are given in Table 6.2.4. Three dimensional cartesian coordinates on the local system have been computed from the geodetic coordinates and are given in Table 6.2.5.

The computation of cartesian coordinates has been done at the surface of the reference ellipsoid in both cases (Arc-Datum 1960 and WGS84). This is because;

- The orthometric heights given are only approximate (obtained by trigonometric heighting).
- The GPS heights were taken from different points due to vandalism of some pillars.
- The orthometric heights cannot be taken as the ellipsoidal heights for the local datum because the average geoidal undulation in Kenya is 290m (*Mwakuchengwa, 1994*).

It should be noted however that the local datum referred to here is based on modified Clarke 1880 reference ellipsoid.

Table 6.2.1: WGS84 ellipsoidal curvilinear coordinates of the triangulation points

| Point code | ϕ (° ' ") (S) | λ (° ' ") (E) | h (m) |
|------------|--------------------|-----------------------|-----------|
| 148 s1 | 01 03 13.8872 | 36 46 21.2925 | 1983.0923 |
| 149 s2 | 01 06 10.8720 | 37 06 47.4987 | 1485.4813 |
| 149 s3 | 01 28 16.3236 | 37 03 47.6416 | 1822.6452 |
| 148 st5 | 01 29 26.9309 | 36 37 04.903 | 1847.1834 |
| 148 st6 | 01 19 05.1201 | 36 33 00.3459 | 1861.6813 |
| 148 s2 | 01 10 00.9150 | 36 46 38.2578 | 1889.9532 |
| 148 s4 | 01 13 32.4980 | 36 54 54.3169 | 1571.6542 |

Table 6.2.2: WGS84 ellipsoidal cartesian coordinates of the triangulation points

| Point code | X (m) | σ_X (m) | Y (m) | σ_Y (m) | Z (m) | σ_Z (m) |
|------------|-------------|----------------|-------------|----------------|--------------|----------------|
| 148S1 s1 | 5108143.752 | ±0.0036 | 3817568.580 | ±0.0056 | -1165 23.098 | ±0.0013 |
| 149S2 s2 | 5085277.292 | ±0.0032 | 3847806.180 | ±0.0031 | -121985.256 | ±0.0010 |
| 149 s3 | 5087900.809 | ±0.0026 | 3842819.347 | ±0.0025 | -162659.467 | ±0.0012 |
| 148 st5 | 5117561.776 | ±0.0016 | 3083135.798 | ±0.0013 | -164827.466 | ±0.0005 |
| 148 st6 | 5107635.686 | ±0.0027 | 3817843.664 | ±0.0022 | -129022.686 | ±0.0008 |
| 148 s2 | 5122443.397 | ±0.0060 | 3797344.290 | ±0.0093 | -145734.130 | ±0.0022 |
| 148 s4 | 5098330.672 | ±0.0038 | 3830034.787 | ±0.0059 | -135520.083 | ±0.0016 |

Table 6.2.3: Local UTM plane coordinates and orthometric heights of the triangulation points

| Point code | N (m) | E (m) | H (m) |
|------------|----------------|--------------|-----------|
| 148 s1 | 9 883 726. 885 | 252 026. 265 | 1999.3970 |
| 149 s2 | 9 878 315. 023 | 289 949. 592 | 1501.0181 |
| 149 s3 | 9 837 592. 787 | 284 419. 100 | 1838.3710 |
| 148 st5 | 9 835 375. 070 | 234 861. 940 | 1860.1942 |
| 148 st6 | 9 854 475. 770 | 227 278. 510 | 1874.5200 |
| 148 s2 | 9 871 220. 857 | 252 560. 376 | 1906.6915 |
| 148 s4 | 9 864 732. 064 | 267 906. 109 | 1588.5143 |

Table 6.2.4: Local geodetic coordinates of the triangulation points

| Point code | ϕ (° ' ") (S) | λ (° ' ") (E) |
|------------|--------------------|-----------------------|
| 148 s1 | 01 03 04.5161 | 36 46 18.3166 |
| 149 s2 | 01 06 01.5155 | 37 06 44.4997 |
| 149s3 | 01 28 07.0888 | 37 03 44.6476 |
| 148 st5 | 01 29 17.7046 | 36 37 01.9396 |
| 148 st6 | 01 18 55.8374 | 36 32 57.3869 |
| 148 s2 | 01 09 51.5812 | 36 46 35.2822 |
| 148 s4 | 01 13 23.1828 | 36 54 51.3321 |

The local geodetic coordinates in Table 6.2.4 have been computed via the iterative method as discussed in section (4.3.3). It was in the interest of this research to check the above results by determining the geodetic coordinates of one of the points (148 st5) by the use of conventional UTM tables. The following results were obtained, $\phi = -01^{\circ} 29' 17.7045''$ and $\lambda = 36^{\circ} 37' 01.9322''$. It can be seen that the differences between the iterated values and the values determined via UTM tables are not significant. However, it should be noted that the absolute difference in the values of ϕ is $0''.0001$ while that of λ is $0''.0074$. This shows that the conventional UTM tables may equally be useful though tedious.

Table 6.2.5: Local ellipsoidal cartesian coordinates of the triangulation points

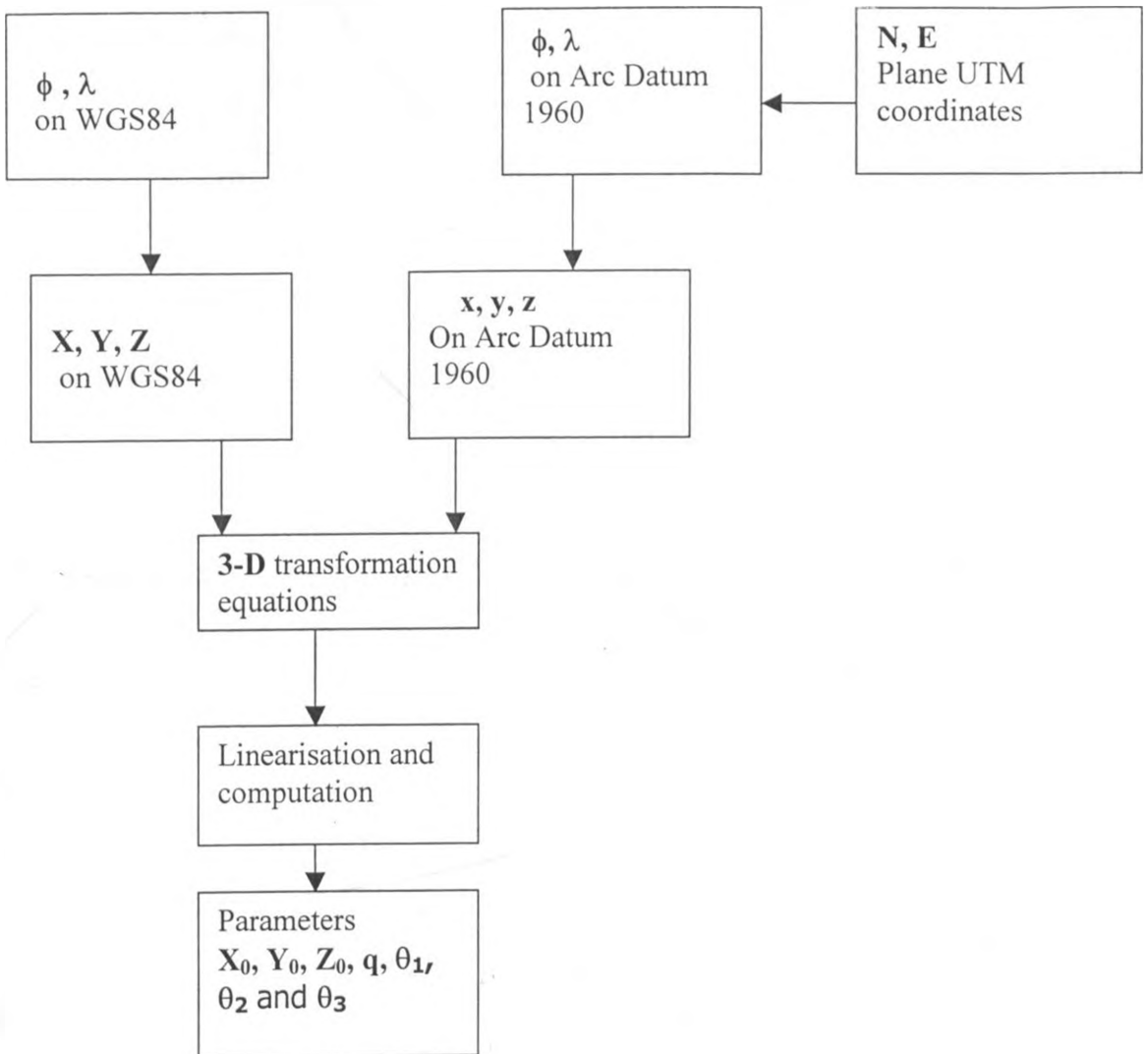
| Point | X(m) | Y (m) | Z (m) |
|---------|---------------|---------------|--------------|
| 148 s1 | 5 108 292.975 | 3 817 565.238 | -116 224.587 |
| 149 s2 | 5 085 427.160 | 3 847 807.307 | -121 659.695 |
| 149 s3 | 5 088 052.037 | 3 842 817.583 | -162 360.932 |
| 148 st5 | 5 117 712.488 | 3 803 133.685 | -164 528.995 |
| 148 st6 | 5 107 785.356 | 3 817 840.684 | -128 724.177 |
| 148 s2 | 5 122 593.351 | 3 797 341.582 | -145 435.665 |
| 148s4 | 5 098 480.741 | 3 830 032.213 | -135 221.576 |

6.3 Determination of Transformation Parameters

The determination of seven transformation parameters between WGS84 and Arc-Datum 1960 coordinates is accomplished by three dimensional similarity transformation equations (Bursa-Wolf model). In this case the axes of the local and global systems are taken to be non parallel. hence a requirement to bring them into parallelism via rotations θ_1 , θ_2 and θ_3 about X-, Y- and

Z- axes respectively. X_0 , Y_0 and Z_0 are the datum shifts while q is the uniform scale change. Figure 6.3.1 below shows the procedure(s) involved in this determination.

Figure 6.3.1: Flow chart showing determination of seven transformation parameters



6.4 GPS/Lev Points

The GPS/Lev points are within the triangulation network used for the determination of transformation parameters. The GPS coordinates (geodetic: – latitudes and longitudes) are given in Table 6.4.1 while GPS heights (geodetic heights), orthometric heights and geoidal undulations of the same points are given in Table 6.4.2. The spatial distribution of the GPS/Lev points is given in Figure 6.4.1.

Table 6.4.1: GPS coordinates (geodetic: - latitudes and longitudes) of the GPS/Lev points

| Point name/code | ϕ (° ' ") (S) | λ (° ' ") (E) |
|-----------------|--------------------|-----------------------|
| V/33 | 01 10 43.64460 | 36 38 54.95361 |
| Vet farm X | 01 20 10.46989 | 36 39 38.93290 |
| V/20 | 01 17 20.70609 | 36 41 08.23685 |
| VA/9 | 01 14 18.04136 | 36 40 29.02277 |
| IN37 | 01 17 55.51984 | 36 45 37.97528 |
| 148t19 | 01 23 29.20534 | 36 46 24.34763 |
| V/6 | 01 18 11.59437 | 36 49 24.79764 |
| 148 s3 | 01 07 59.58027 | 36 58 23.87527 |
| IV/13 | 01 25 17.72190 | 36 56 51.22002 |
| 37 | 01 14 38.65885 | 36 52 03.27169 |
| Kism 7X | 01 09 33.56783 | 36 52 53.83311 |
| LXI 14 | 01 15 29.00837 | 36 54 03.12382 |
| IV/10 | 01 21 01.37710 | 36 53 37.41441 |
| Marulais | 01 13 32.49800 | 36 54 54.31690 |
| Kism | 01 15 00.77709 | 36 51 24.03884 |
| V/7 | 01 18 23.95868 | 36 48 44.86614 |
| MT3 | 01 13 34.97585 | 36 53 00.23718 |
| Stigands X | 01 24 07.26869 | 36 56 40.17275 |

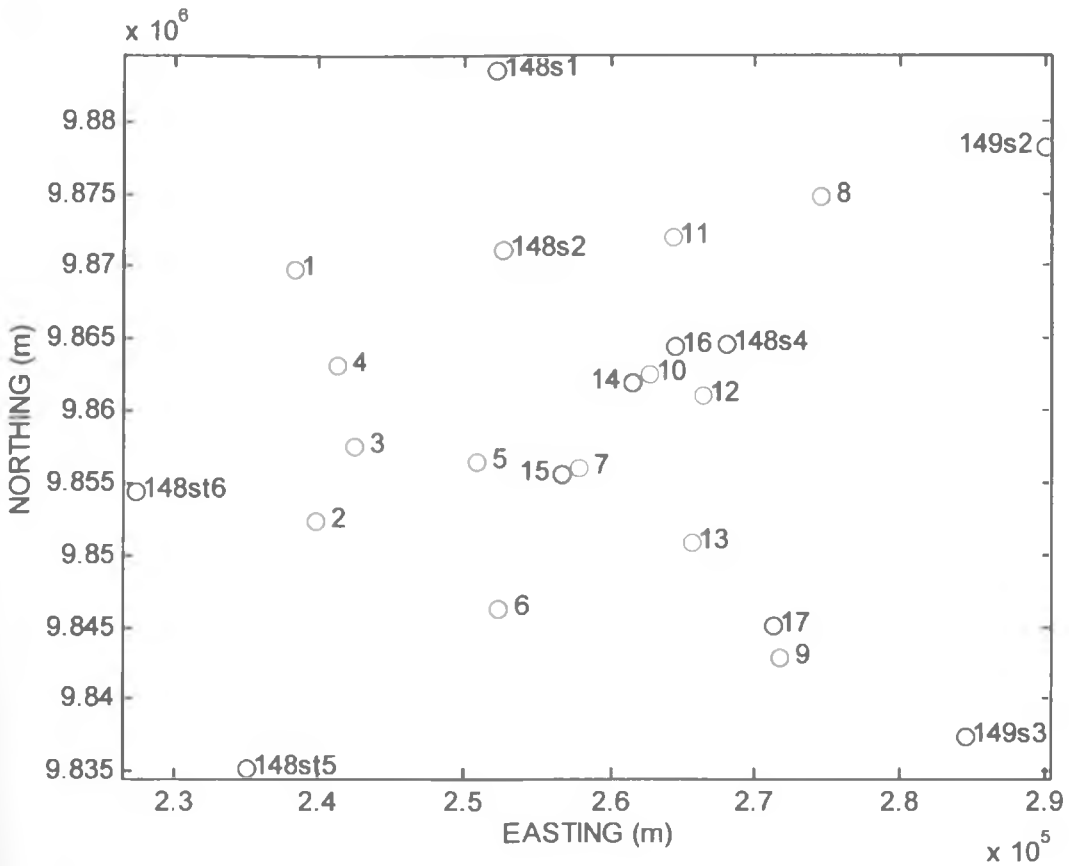
Table 6.4.1: GPS coordinates (geodetic: - latitudes and longitudes) of the GPS/Lev points

| Point name/code | ϕ (° ' ") (S) | λ (° ' ") (E) |
|-----------------|--------------------|-----------------------|
| V/33 | 01 10 43.64460 | 36 38 54.95361 |
| Vet farm X | 01 20 10.46989 | 36 39 38.93290 |
| V/20 | 01 17 20.70609 | 36 41 08.23685 |
| VA/9 | 01 14 18.04136 | 36 40 29.02277 |
| IN37 | 01 17 55.51984 | 36 45 37.97528 |
| 148t19 | 01 23 29.20534 | 36 46 24.34763 |
| V/6 | 01 18 11.59437 | 36 49 24.79764 |
| 148 s3 | 01 07 59.58027 | 36 58 23.87527 |
| IV/13 | 01 25 17.72190 | 36 56 51.22002 |
| 37 | 01 14 38.65885 | 36 52 03.27169 |
| Kism 7X | 01 09 33.56783 | 36 52 53.83311 |
| LXI 14 | 01 15 29.00837 | 36 54 03.12382 |
| IV/10 | 01 21 01.37710 | 36 53 37.41441 |
| Marulais | 01 13 32.49800 | 36 54 54.31690 |
| Kism | 01 15 00.77709 | 36 51 24.03884 |
| V/7 | 01 18 23.95868 | 36 48 44.86614 |
| MT3 | 01 13 34.97585 | 36 53 00.23718 |
| Stigands X | 01 24 07.26869 | 36 56 40.17275 |

Table 6.4.2: Geodetic heights, orthometric heights and geoidal undulations of the GPS/Lev points.

| Point name/code | Ellipsoidal height | Orthometric height | Geoid height | Plotting code |
|------------------------|---------------------------|---------------------------|---------------------|----------------------|
| V/33 | 2127.7173 | 2144.1857 | -16.4684 | 1 |
| Vet farm | 1918.1333 | 1934.5859 | -16.4526 | 2 |
| V/20 | 1877.9951 | 1894.6856 | -16.6905 | 3 |
| VA/9 | 1979.6083 | 1996.1291 | -16.5208 | 4 |
| IN37 | 1777.9858 | 1794.6261 | -16.6403 | 5 |
| 148t19 | 1699.5543 | 1716.2024 | -16.6481 | 6 |
| V/6 | 1645.0073 | 1661.8351 | -16.8278 | 7 |
| 148s2 | 1889.9532 | 1906.6915 | -16.7383 | 148s2 |
| 148s3 | 1517.4503 | 1534.3873 | -16.9370 | 8 |
| IV/13 | 1532.5783 | 1549.5392 | -16.9609 | 9 |
| 37 | 1603.7949 | 1620.7161 | -16.9212 | 10 |
| Kism 7X | 1573.7616 | 1590.4891 | -16.7275 | 11 |
| LXI 14 | 1580.1454 | 1596.9813 | -16.8359 | 12 |
| IV/10 | 1619.8719 | 1636.6663 | -16.7944 | 13 |
| Marulais | 1571.6542 | 1588.5143 | -16.8601 | 148s4 |
| Kism | 1628.4483 | 1645.2696 | -16.8213 | 14 |
| V/7 | 1663.3580 | 1680.1003 | -16.7423 | 15 |
| MT3 | 1594.5000 | 1611.3359 | -16.8359 | 16 |
| Stigands X | 1573.3818 | 1590.1980 | -16.8162 | 17 |

Figure 6.4.1: Spatial distribution of the GPS/Lev points within the triangulation network

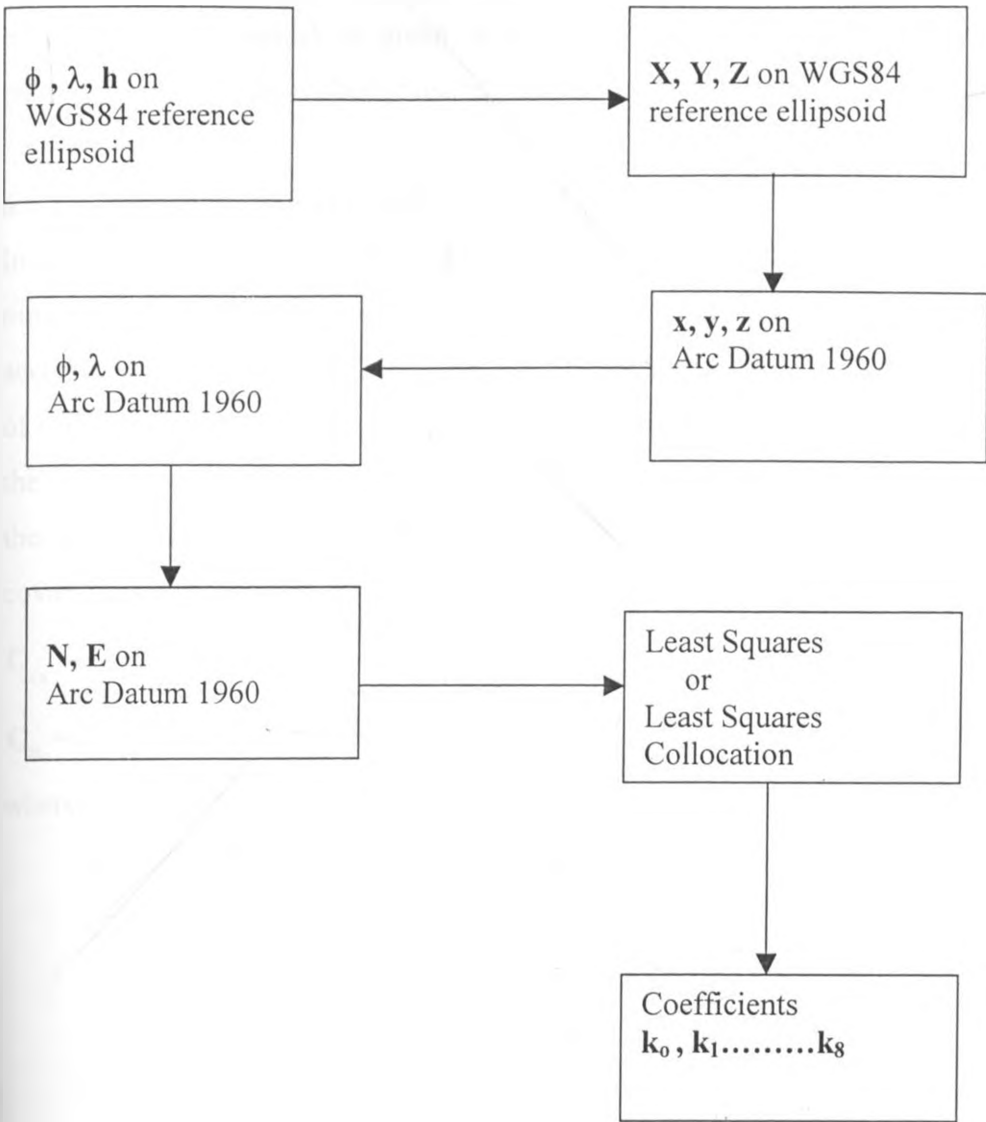


From the diagram above, points 1-13 and 148s2 have been used for the computation of the biquadratic polynomial while points 14 to 17 and 148s4 have been used for testing the polynomial. The plotting codes in Table 6.4.2 have been used to represent point names/codes in Figure 6.4.1.

6.5 Polynomial Determination

The biquadratic polynomial equation (2.2.3-2) has been used in this study. The coefficients have been determined via the Least Squares and Least Squares Collocation techniques. Fourteen GPS/Lev points have been used for the determination of nine coefficients of the polynomial. The general computation procedure is given in Figure 6.5.1.

Figure 6.5.1: Flow chart showing determination of the coefficients of the polynomial



In the above flow chart, the observed WGS84 geodetic coordinates are transformed into WGS84 cartesian coordinates. The cartesian coordinates on WGS84 are transformed into the local cartesian coordinates via the seven transformation parameters. The local cartesian coordinates are transformed into the local geodetic coordinates, which are then projected onto a plane via UTM projection equations to obtain the local plane coordinates. The local plane coordinates together with geoid heights (h-H) are then used in the quadratic polynomial equation to obtain coefficients through either Least Squares or Least Squares Collocation techniques. The coefficients obtained by the two techniques are given in chapter seven.

6.5.1 Determination of Coefficients by Least Squares

The simple Gauss Markov model has been used to determine the nine coefficients of the polynomial. The model is given in equation 5.4-3. The accuracies of the approximated parameters have been evaluated using equation 5.5-1.

6.5.2 Determination of Coefficients by Least Squares Collocation

In Least Squares Collocation equation (2.2.1-16) has been used for the determination of the nine coefficients of the quadratic polynomial. The interpolation of geoidal heights is accomplished by equation (2.2.1-19). The covariance matrix C_{nn} is obtained from the accuracy of the observations with the assumption of no correlation. The covariance of the signal part of the observation is obtained by equation (6.5.2-1) while the covariance for the random part at the interpolation points is evaluated via equation (6.5.2-2). The constants (C_0 and a) of the covariance function are approximated from the accuracy of the signal data.

$$C_{s's'} = C_0 e^{-a^2 r^2} \quad (6.5.2 - 1)$$

$$C_{ss} = C_0 e^{-a^2 r^2} \quad (6.5.2 - 2)$$

where,

$C_{s's'}$ is covariance of noise in the signal part of the observation

C_{ss} is covariance of the random part

r is distance between observation points (6.5.2-1) or distance between interpolation points (6.5.2-2)

C_0 and a are constants.

The cross covariance between observations and signals is given as;

$$C_{ys} = C_0 e^{-a^2 r^2} \quad (6.5.2 - 3)$$

where,

C_{ys} is cross covariance from signal to observation points

r is distance between observation and signal points

C_0 and a – are constants

Now

$$\bar{C} = C_{yy} = C_{nn} + C_{s's'} \quad (6.5.2 - 4)$$

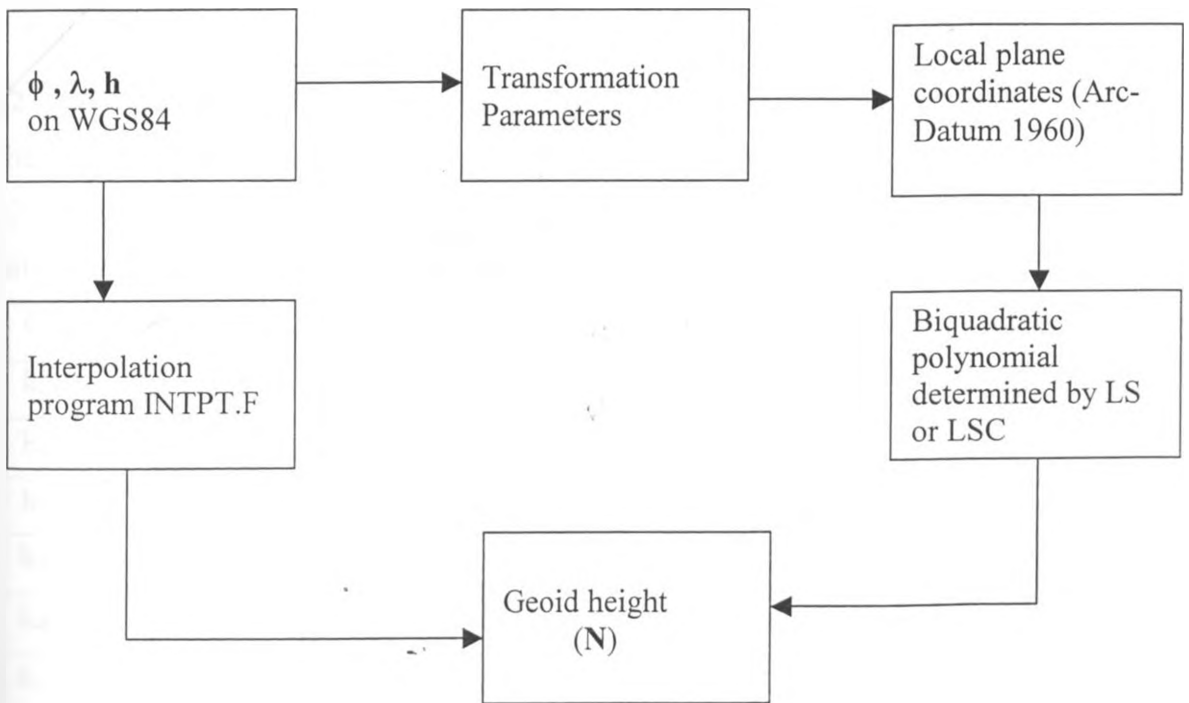
and $C_{sy} = C_{ys}^T$. (6.5.2 - 5)

The covariance \bar{C} is used for the determination of coefficients and their accuracies in equations (2.2.1-16) and (2.2.1-20) respectively. Both \bar{C} and C_{sy} are used in the determination of signals (interpolation) in equation (2.2.1-19) while all the covariances \bar{C} , C_{sy} and C_{ss} are exploited in the computation of the accuracy estimates of signals in equation (2.2.1-21).

6.6 Interpolation of Geoid Heights

Having obtained transformation parameters and coefficients of the biquadratic polynomial in the area of study, it is now possible to obtain geoid height of a point in the area covered by the polynomial. Three methods have been used for the interpolation of geoid heights, these include; biquadratic polynomial (determined by LS and LSC) and a gridded representation of EGM96 through a bilinear interpolation program INTPT.F as given in Figure (6.6.1). From the geoid heights and the geodetic heights, orthometric heights can be derived.

Figure 6.6.1: Flow chart showing interpolation of geoid heights



CHAPTER SEVEN

RESULTS AND ANALYSIS

7.1 Transformation Parameters

The computed transformation parameters and their accuracies are given in Table 7.1.1.

Table 7.1.1: Transformation parameters

| Parameter | Bursa-Wolf model | | Molodensky model | | Units |
|----------------|------------------|-----------------------------|------------------|----------|-------|
| | Value | Accuracy | Value | Accuracy | |
| X ₀ | -150.105 | - | -150.104 | ± 0.001 | m |
| Y ₀ | 2.634 | - | 2.635 | ± 0.001 | m |
| Z ₀ | -298.512 | - | -298.512 | ± 0.000 | m |
| q | 0.999999948 | ± 2.4920 × 10 ⁻⁸ | | | - |
| θ ₁ | 0.257596 | ± 0.4461 | | | " |
| θ ₂ | 0.192634 | ± 0.3334 | | | " |
| θ ₃ | -0.004647 | ± 0.0140 | | | " |

7.2 Polynomial Coefficients by Least Squares

The evaluated coefficients of the biquadratic polynomial by Least Squares are given in Table 7.2.1.

Table 7.2.1: Coefficients by Least Squares.

| Coefficient | Value | Accuracy | Units |
|----------------|-------------------------------|--------------------------------|-----------------|
| k ₀ | 0.000000 | ±0.000000 | m |
| k ₁ | -7.600000 × 10 ⁻²⁹ | ±8.700000 × 10 ⁻³² | - |
| k ₂ | 0.000000 | ±0.000000 | - |
| k ₃ | -1.244425 × 10 ⁻²⁵ | ±1.261432 × 10 ⁻²⁷ | m ⁻¹ |
| k ₄ | -9.551580 × 10 ⁻²⁴ | ±9.682114 × 10 ⁻²⁶ | m ⁻¹ |
| k ₅ | -4.120000 × 10 ⁻²⁹ | ±4.180000 × 10 ⁻³¹ | m ⁻¹ |
| k ₆ | -1.219639 × 10 ⁻¹⁸ | ±1.236307 × 10 ⁻²⁰ | m ⁻² |
| k ₇ | -2.034024 × 10 ⁻²² | ±2.0618216 × 10 ⁻²⁴ | m ⁻² |
| k ₈ | 2.136800 × 10 ⁻²⁴ | ±4.864115 × 10 ⁻²⁶ | m ⁻³ |

7.2.1 Application of Polynomial coefficients by LS on Test Data

The determined coefficients of the biquadratic polynomial given in Table 7.2.1 were used to interpolate for the geoid heights at five test points. The results are given in Table 7.2.1.1.

Table 7.2.1.1: Interpolated geoid heights by polynomial (LS) at the test points

| Test Point | Geoid Height (m) | Plotting code |
|------------|------------------|---------------|
| Marulais | -16.8725 | 148s4 |
| Kism | -16.8072 | 14 |
| V/7 | -16.7319 | 15 |
| MT3 | -16.8440 | 16 |
| Stigands X | -16.8275 | 17 |

7.3 Polynomial Coefficients by Least Squares Collocation

The evaluated coefficients of the biquadratic polynomial by Least Squares Collocation are given in Table 7.3.1.

Table 7.3.1: Coefficients by Least Squares Collocation

| Coefficient | Value | Accuracy | Units |
|-------------|-----------------------------|--------------------------------|----------|
| k_0 | 0.000000 | ± 0.000000 | m |
| k_1 | $-9.670000 \times 10^{-29}$ | $\pm 6.890000 \times 10^{-32}$ | - |
| k_2 | 0.000000 | ± 0.000000 | - |
| k_3 | $-1.244303 \times 10^{-25}$ | $\pm 8.847746 \times 10^{-27}$ | m^{-1} |
| k_4 | $-9.551006 \times 10^{-24}$ | $\pm 6.791344 \times 10^{-26}$ | m^{-1} |
| k_5 | $-4.090000 \times 10^{-29}$ | $\pm 2.897000 \times 10^{-31}$ | m^{-1} |
| k_6 | $-1.219612 \times 10^{-18}$ | $\pm 8.672177 \times 10^{-21}$ | m^{-2} |
| k_7 | $-2.010083 \times 10^{-22}$ | $\pm 1.429291 \times 10^{-24}$ | m^{-2} |
| k_8 | 2.136739×10^{-24} | $\pm 3.074353 \times 10^{-26}$ | m^{-3} |

7.3.1 Application of polynomial coefficients by LSC on Test Data

The determined coefficients of the biquadratic polynomial given in Table 7.3.1 were used to interpolate for the signals (geoid heights) at the five test points. Least Squares Collocation technique was used for the interpolation and the results are given in Table 7.3.1.1.

Table 7.3.1.1: Interpolated geoid heights by polynomial (LSC) at the test points.

| Test Point | Geoid Height (m) | Accuracy (m) | Plotting code |
|------------|------------------|--------------|---------------|
| Marulais | -16.8724 | ± 0.0536 | 148s4 |
| Kism | -16.8072 | ± 0.0536 | 14 |
| V/7 | -16.7320 | ± 0.0536 | 15 |
| MT3 | -16.8439 | ± 0.0536 | 16 |
| Stigands X | -16.8278 | ± 0.0536 | 17 |

7.4 Application of EGM96 on Test Data

The EGM96 was used to obtain geoidal undulations at the test points. The results are given in Table 7.4.1.

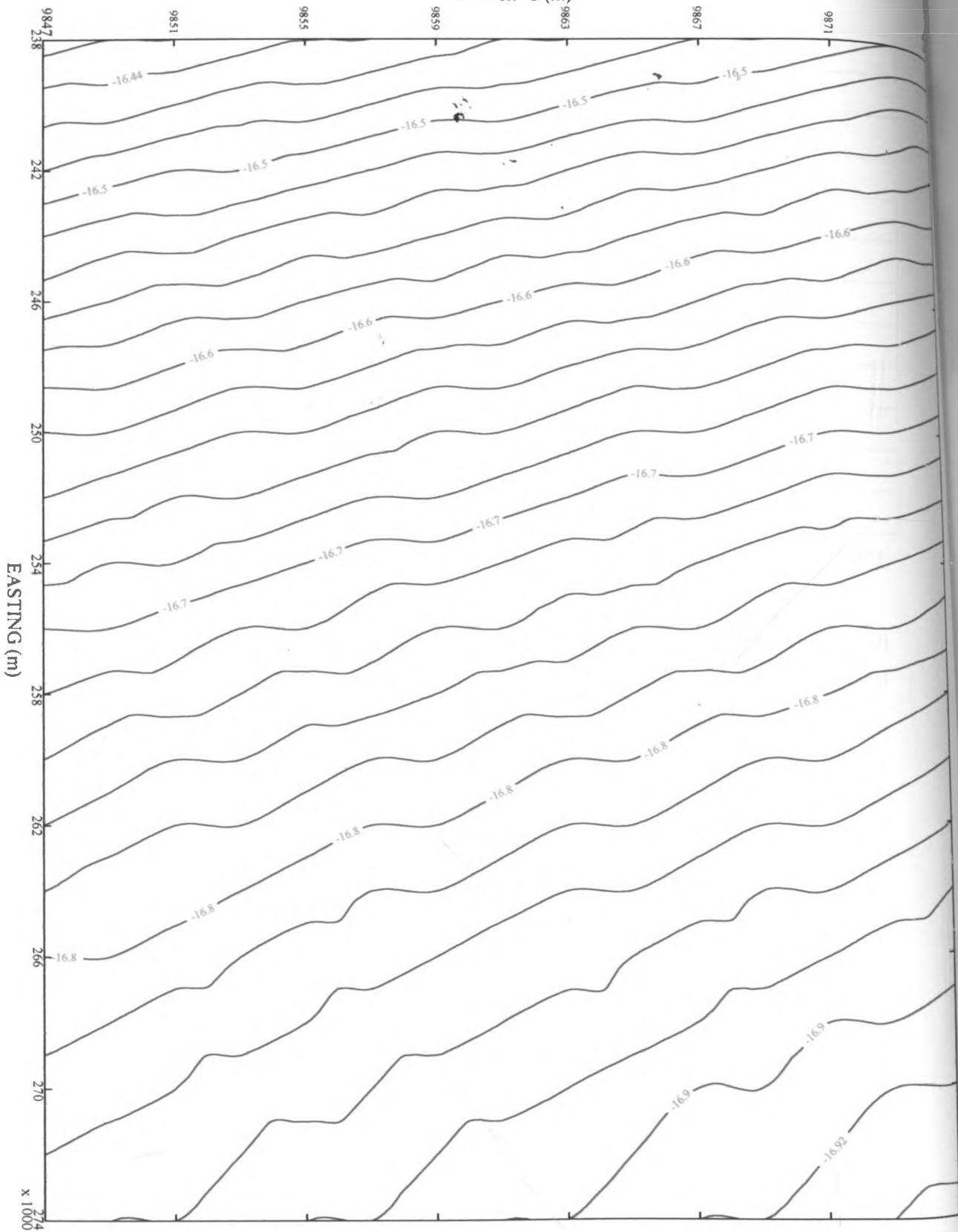
Table 7.4.1: Interpolated geoid heights by EGM96 at the test points

| Test Point | Geoid Height (m) | Plotting code |
|------------|------------------|---------------|
| Marulais | -15.90 | 148s4 |
| Kism | -15.94 | 14 |
| V/7 | -16.08 | 15 |
| MT3 | -15.90 | 16 |
| Stigands X | -15.90 | 17 |

7.5 The Nairobi Area Geoid

The Nairobi area geoid was interpolated by the biquadratic polynomial on a 2 km square grid. Contours of geoid heights were then interpolated at 2 cm vertical interval via Professional - Surveyor Plus software. The resulting Nairobi area geoid with respect to WGS84 reference ellipsoid is shown in Figure 7.5.1. It should be noted that the geoid heights are in metres.

NORTHING (m)



x 1000

7.6 Analysis

The computed transformation parameters (X_0 , Y_0 , Z_0) obtained by Bursa-Wolf model are reasonable but their accuracies are unrealistically small while the scale factor (q) does not deviate significantly from unity. However, the rotation parameters (θ_1 , θ_2 and θ_3) are very small and further smaller than their standard errors. This scenario can be attributed to either the size of the area used (difficulty in detecting the curvature of the earth on a small fraction of the earth) or parallelism of the axes of the two datums (Arc- Datum 1960 and WGS84). That being the case then the three translations alone are enough to model the transformation. Molodensky model is therefore adopted.

The coefficients of the biquadratic polynomial determined by LS and LSC have almost the same values and accuracies. This may be attributed to the low quality of the covariance function used due to lack of sufficient data in Least Squares Collocation otherwise LSC is expected to perform better than LS. The computed residuals at data points show no significant difference between LS and LSC fit at the 14 data points as given in Table 7.6.1 although data points 3, 9, 10, and 11 are found to have larger residuals. This is however consistent with the low accuracy (6 – 8cm) of height determination at the same points (3, 9, 10, and 11).

Table 7.6.1: Residuals obtained by LS and LSC at the data points

| Data point | Residual (m) | | Difference (m) |
|------------|--------------|---------|----------------|
| | LS | LSC | |
| 1 | 0.0225 | 0.0221 | 0.0001 |
| 2 | 0.0067 | 0.0063 | 0.0004 |
| 3 | -0.1629 | -0.1633 | 0.0004 |
| 4 | 0.0035 | 0.0031 | 0.0004 |
| 5 | 0.0183 | 0.0179 | 0.0004 |
| 6 | -0.0038 | -0.0042 | 0.0004 |
| 7 | -0.0801 | -0.0804 | 0.0003 |
| 148s2 | -0.0043 | -0.0047 | 0.0004 |
| 8 | 0.0090 | 0.0087 | 0.0003 |
| 9 | -0.1388 | -0.1391 | 0.0003 |
| 10 | -0.0999 | -0.1002 | 0.0004 |

Continuation of residuals obtained by LS and LSC at the data points

| Data point | Residual (m) | | Difference (m) |
|------------|--------------|--------|----------------|
| 11 | 0.1401 | 0.1397 | 0.0004 |
| 12 | 0.0124 | 0.0120 | 0.0004 |
| 13 | 0.0126 | 0.0123 | 0.0003 |

To analyse geoid heights obtained by the three methods, orthometric and geodetic heights of test points have been used to obtain the 'best' approximated geoid heights ($h - H$) upon which the interpolated geoid heights by the three methods are assessed. The differences between the 'best' approximated geoid height ($h - H$) and the other geoid heights for every test point are given in Table 7.6.2.

Table 7.6.2: Differences of geoid heights

| Test Point / Plotting code | $N_{Geo} - N_{LS}$ (m) | $N_{Geo} - N_{LSC}$ (m) | $N_{Geo} - N_{EGM96}$ (m) |
|----------------------------|------------------------|-------------------------|---------------------------|
| Marulais / (148s4) | +0.0124 | +0.0123 | -0.9601 |
| Kism / (14) | -0.0141 | -0.0141 | -0.8813 |
| V/7 / (15) | -0.0104 | -0.0103 | -0.6623 |
| MT3 / (16) | +0.0081 | +0.0080 | -0.9359 |
| Stigands X / (17) | +0.0113 | +0.0116 | -0.9162 |
| Min abs diff | 0.0081 | 0.0080 | 0.6623 |
| Max abs diff | 0.0141 | 0.0141 | 0.9601 |
| Mean of diff | +0.0015 | +0.0015 | -0.8712 |
| RMS | ± 0.0114 | ± 0.0114 | ± 0.8778 |
| Sd | ± 0.0113 | ± 0.0113 | ± 0.1075 |

where,

N_{Geo} is the geoid height obtained as ($h - H$),

N_{LS} is the geoid height obtained by biquadratic polynomial determined by LS technique,

N_{LSC} is the geoid height obtained by biquadratic polynomial determined by LSC technique,

N_{EGM96} is the geoid height obtained by EGM96 (a bilinear interpolation program INTPT.F),

Sd is standard deviation, and RMS is root mean square.

From Table 7.6.2 it is observed that the geoid heights obtained by polynomial (coefficients determined by LS and LSC) compare favourably on the test points with root mean square of ± 1 cm, mean difference value of 1.5 mm and standard deviation of ± 1 cm. This accuracy is good enough for most levelling applications (engineering surveying, topographic surveying and other related fields). It is mentioned in *Uren and Price (1994)* that for longitudinal sections, it is sufficiently accurate to record levelling readings to the nearest 1cm. The geoid heights approximated by EGM96 are however found to compare poorly on the test points with root mean square of ± 88 cm, mean difference value of -87 cm and standard deviation of ± 11 cm.

It must be noted however that the interpolated geoid heights obtained by Least Squares Collocation have stochastic parameters (standard errors). Hence for data integration, Least Squares Collocation gives a better format of the geoid height solution although LS technique is easier to use and relatively accurate when using one set of data. The EGM96 is suitable only for rough approximation of the geoid height at any point of the earth surface.

The biquadratic polynomial can therefore be used for geoid interpolation in a small area. However for a large area (country or continent) a bicubic polynomial should be considered. This is because the change in slope of the geoid to the reference ellipsoid in a small area is generally uniform and gentle as opposed to a larger area. The biquadratic polynomial is also found to perform better than bilinear polynomial in the area of study.

CHAPTER EIGHT

CONCLUSIONS AND RECOMMENDATIONS

8.1 Conclusions

The Nairobi area geoid has been determined through the orthometric and ellipsoidal heights. The geoid heights increase eastwards in the area of study. For the interpolation of geoid heights in the area of study, a biquadratic polynomial has been used. It is observed that the biquadratic polynomial (determined via LS and LSC) gives a better prediction of geoid heights than EGM96 (a bilinear interpolation program INTPT.F). RMS and Sd for the differences between observed and predicted values at the test points are equal i.e. $\pm 1\text{cm}$ for the biquadratic polynomial (obtained by LS and LSC).

The geoid height has been expressed as a function of the plane local coordinates for easier integration into the local applications. It is found that the local geoid in Nairobi is below the reference ellipsoid (WGS84) with a mean height of -16.75m . This is better than the local datum, which on average deviates from the geoid by as much as 290m over the entire country (Kenya). The WGS84 reference ellipsoid therefore approximates the geoid over Nairobi area better than the local datum (Arc-Datum 1960) based on the modified Clarke 1880 reference ellipsoid.

It is noted that the geoid as determined is a local geoid. It may deviate from the global geoid (actual geoid) by as much as $\pm 2\text{m}$. This is because the mean value of the local mean sea level has been used as the reference surface for orthometric heights. The local mean sea level has however been and is still being used for most if not all survey work the world over. The determined geoid is therefore good enough for local survey work.

It was also in the interest of this research to make the use of the determined geoid possible for local topographic and engineering surveying. It is appreciated that most if not all of the survey work in Nairobi area have been done in the local coordinate system (Arc - Datum 1960). Hence the need for the determination of transformation parameters between WGS84 and Arc - Datum 1960. The transformation parameters determined by Molodensky model are adequate while the parameters obtained by Bursa-Wolf model are found to be unstable. This may be attributed to either the size of the area used (difficulty in detecting the curvature of the earth on

a small fraction of the earth) or parallelism of the axes of the two datums (Arc-Datum 1960 and WGS84). The application of the transformation parameters determined by Molodensky model was found to be satisfactory as they give local coordinates to sub-meter level compared to the local values determined by conventional methods.

A MATLAB program (RUN.M) has been developed to convert the GPS heights into orthometric heights in Nairobi area. The program can also facilitate the use of GPS for local surveying and engineering work in the area of study. The program is made user friendly via the user interface. The user is only required to give the observed GPS data (geodetic – latitude, longitude and height on WGS 84 system). The program then uses the transformation parameters and the polynomial to determine the local plane coordinates (Northing and Easting), geoid height and orthometric height. It is however useful to note that both transformation parameters and the polynomial can only be used for interpolation within the area of coverage. However, with little modifications this program can be used in any other area with a different set of data. GPS survey for local work is now possible in Nairobi area. It will however be interesting to find out how a GPS traverse and levelling networks perform in the area of study.

8.2 Recommendations.

The following are the recommendations arising from this research.

- The accuracy of the determined local geoid may be improved by incorporating a geopotential model and local terrain information. This would require a digital terrain model of the area of study.
- A combination of gravimetric and geometric geoid determination is proposed as a possible method that can lead to precise geoid determination in the Nairobi area.
- The difficulty in determining the rotational parameters by Bursa-Wolf model may be attributed to either the small size of the area used or parallelism of the axes in the two datums. It is proposed that the area be increased so as to obtain a more comprehensive conclusion about the axes of the two datums.
- The standard errors of Arc Datum 1960 coordinates have been unrealistically assumed to be zero. This is not true because coordinates are computed from observations that are stochastic in nature. The triangulation network should be recomputed from the original observations to enable the determination of stochastic parameters of the coordinates.

A further study should then be carried out to consider an estimation model that incorporates stochastic parameters of coordinates in the two systems for better solution of the transformation parameters.

APPENDICES

APPENDIX A: PRELIMINARY COMPUTATION PROGRAM

%This program computes local geodetic coordinates from the
%local plane UTM coordinates.

%Elements of modified Clarke1880 reference ellipsoid.

a1=6378249.145; %semi major axis.
f1=1/293.465; %ellipticity.
e1=sqrt(2*f1-f1^2); %first eccentricity.

N=input(' Northing Value ');

E=input(' Easing Value ');

e2=(2*f1-f1*f1);

K=0.9996;

dn=10000000-N;

de=500000-E;

R=6371000;

La=dn/R;

VO=a1/(sqrt(1-e2*sin(La)^2));

Lo=de/(VO*cos(La));

n=f1/(2-f1);

co=1+n^2/4+n^4/64;

c12=3/2*(n-n^3/8);

c14=15/16*(n^2-n^4/4);

c16=35/48*n^3;

c18=315/512*n^4;

```

for i=1:15;
VO=a1/(sqrt(1-e2*sin(La)^2)); %radius in the prime vertical.
so=a1/(1+n)*(co*La-c12*sin(2*La)+c14*sin(4*La)-
c16*sin(6*La)+c18*sin(8*La));
%so is the meridional distance.
ro=a1*(1-e2)/(1-e2*(sin(La))^2)^1.5; %radius in the meridian.
N1=((VO/2)*(Lo*cos(La))^2*tan(La))+((VO/24)*(Lo*cos(La))^4*tan(
La)*(5-(tan(La))^2));
NL=K*(so+N1);
EL=K*((VO*Lo*cos(La))+(((VO/6)*(Lo*cos(La))^3)*((VO/ro)-
(tan(La))^2))+((VO/120)*(Lo*cos(La))^5*(5-
18*(tan(La))^2+(tan(La))^4)));

dN=dn-NL;
dE=de-EL;

dLa=dN/ro;
dLo=dE/(VO*cos(La));

La=(dLa+La);
Lo=(dLo+Lo);
end;

disp('      ')
disp('      ')
disp('Latitude and Longitude in degrees');
Latitude =-(La*180/pi)      %Computed latitude in degrees.
Longitude=39-Lo*180/pi     %Computed longitude in degrees.

```


APPENDIX B: MAIN PROGRAM (RUN.M)

```

disp(' ');
disp(' ');
disp('This program determines: transformation parameters,
polynomial coefficients,')
disp('geoid heights, local plane coordinates and orthometric
heights')
disp(' ');
disp('By Patroba A Odera.')
```

```

disp(' ');
disp(' ');
disp('USER INTERFACE');
```

```

disp('*****
***');
disp('PLEASE ENJOY THE PROGRAM');
```

```

disp('*****
**');
disp('THE USER IS REQUIRED TO INPUT THE RIGHT DATA AT THE
PROMPT');
```

```

disp('*****
***');
disp('PLEASE USE THE RIGHT FORMAT AS INDICATED');
```

```

disp('*****
***');
disp('INPUT-LATITUDE(-ve if S), LONGITUDE AND ELLIPSOIDAL
HEIGHT ON WGS84');
```

```

disp('*****
***');
```

```

disp('OUTPUT-N, E ON ARC DATUM1960, GEOID HEIGHT AND ORTHOMETRIC
HEIGHT');
```

```

disp(' ');
disp(' ');
disp('INPUT DATA');
```

```

disp(' ');
clear all
```

```

%DETERMINATION OF TRANSFORMATION PARAMETERS

%Elements of WGS84 reference ellipsoid
aw=6378137;           %semi major axis
fw=1/298.25722356;   %ellipticity
ew=sqrt(2*fw-fw^2); %first eccentricity

%Elements of Clark1880 reference ellipsoid
al=6378249.145;      %semi major axis
fl=1/293.465;        %ellipticity
el=sqrt(2*fl-fl^2); %first eccentricity
```

```

%Constant
    r=206264.806249;

%Reading geodetic coordinates on the global reference
ellipsoid i.e WGS84
%from data file data1.txt.

t1=matin('a:\data1.txt',14,3);
t1=matin('a:\data1.txt',14,3);
N0=size(t1);
N=N0(1);
P=N0(2);

%Reading geodetic coordinates on the local reference ellipsoid
i.e. Clarke 1880
%from data file data2.txt.

t2=matin('a:\data2.txt',N,P);

G=t1;
g=t2;

%Changing degrees to radians

for i=1:N
    gr(i)=(g(i,1)+g(i,2)/60+g(i,3)/3600)*pi/180;
    Gr(i)=(G(i,1)+G(i,2)/60+G(i,3)/3600)*pi/180;
end;

gl=gr';
gw=Gr';

for i=1:N/2
    Vw(i)=aw/(sqrt(1-ew^2*sin(gw(2*i-1))^2)); %radius in the
                                                prime vertical on WGS84
    Vl(i)=al/(sqrt(1-el^2*sin(gl(2*i-1))^2)); %radius in the
                                                prime vertical on Clarke1880
end;

v=Vl';
V=Vw';

%Computing the three-dimensional cartesian coordinates for the
seven points in the
%global and local systems

for i=1:N/2;
    L1(i)= V(i)*cos(gw(2*i-1))*cos(gw(2*i)); % X on WGS84
    L2(i)= V(i)*cos(gw(2*i-1))*sin(gw(2*i)); % Y on WGS84

```

```

L3(i)= V(i)*(1-ew^2)*sin(gw(2*i-1));      % Z on WGS84

L4(i)= v(i)*cos(gl(2*i-1))*cos(gl(2*i)); % x on Clarke1880
L5(i)= v(i)*cos(gl(2*i-1))*sin(gl(2*i)); % y on Clarke1880
L6(i)= v(i)*(1-el^2)*sin(gl(2*i-1));      % z on Clarke1880

end;

L=[L1';L2';L3'];
l=[L4';L5';L6'];

%Rearranging the three dimensional coordinates in the global
and local systems
for i=1:N/2;
    j=i+N/2;
    k=i+N;

c1=3*i-2;
c2=3*i-1;
c3=3*i;

c(c1)=l(i);
c(c2)=l(j);
c(c3)=l(k);

C(c1)=L(i);
C(c2)=L(j);
C(c3)=L(k);

end;

y1=C'; % vector of X,Y,Z coordinates on the global
system(WGS84)
y2=c'; % vector of x,y,z coordinates on the local
system(Clarke1880)

%Computing the approximate parameters(X0,Y0,Z0)using the
seven points

t=y1-y2; %global-local
X0=(t(1)+t(4)+t(7)+t(10)+t(13)+t(16)+t(19))/7;
Y0=(t(2)+t(5)+t(8)+t(11)+t(14)+t(17)+t(20))/7;
Z0=(t(3)+t(6)+t(9)+t(12)+t(15)+t(18)+t(21))/7;

```

MOLODENSKY MODEL (3-PARAMETERS)

```

gd=gw-gl;
df=fw-fl;
da=aw-al;

for i=1:N/2
    Vpv(i)=aw/(sqrt(1-ew^2*sin(gw(2*i-1))^2)); %radius in the
                                                prime vertical
    Vmd(i)=aw*(1-ew^2)/(1-ew^2*(sin(gw(2*i-1)))^2)^1.5;%radius
                                                in the meridian direction
end;

rp=Vpv';
rm=Vmd';
b=aw*(1-fw);
el=sqrt((aw^2-b^2)/b^2); %second eccentricity

%Computing misclosure and design matrix
for i=1:N/2;
    m1(i)=-sin(gw(2*i-1))*cos(gw(2*i-1))*X0/rp(i);
    m2(i)=(-sin(gw(2*i))*cos(gw(2*i-1))*Y0+Z0*cos(gw(2*i-
1)))/rp(i);
    m3(i)=ew^2*sin(gw(2*i-1))*cos(gw(2*i-1))*da/rp(i)*(sqrt(1-
ew^2*sin(gw(2*i-1))^2));
    m4(i)=sin(gw(2*i-1))*cos(gw(2*i-
1))*(2/rp(i))*rm(i)+el^2*(sin(gw(2*i-1)))^2*(1-fw)*df;
    m5(i)=(-X0*sin(gw(2*i))+Y0*cos(gw(2*i)))/(rm(i)*cos(gw(2*i-
1)));

    AA(2*i-1,1)=-sin(gw(2*i-1))*cos(gw(2*i-1))/rp(i);
    AA(2*i-1,2)=(-sin(gw(2*i))*cos(gw(2*i-1))+cos(gw(2*i-
1)))/rp(i);
    AA(2*i-1,3)=cos(gw(2*i-1))/rp(i);
    AA(2*i,1)=-sin(gw(2*i))/rm(i)*cos(gw(2*i-1));
    AA(2*i,2)=cos(gw(2*i))/rm(i)*cos(gw(2*i-1));
end
AA=AA*r;
rT1=(m1'+m2'+m3'+m4'/r);
rT2=m5';
for i=1:N/2;.
    rT(2*i-1)=rT1(i);
    rT(2*i)=rT2(i);
end
yy=gd-rT';

```

MOLODENSKY MODEL (3-PARAMETERS)

```
gd=gw-gl;
df=fw-fl;
da=aw-al;
```

```
for i=1:N/2
    Vpv(i)=aw/(sqrt(1-ew^2*sin(gw(2*i-1))^2)); %radius in the
                                                prime vertical
    Vmd(i)=aw*(1-ew^2)/(1-ew^2*(sin(gw(2*i-1)))^2)^1.5;%radius
                                                in the meridian direction
end;
```

```
rp=Vpv';
rm=Vmd';
b=aw*(1-fw);
e1=sqrt((aw^2-b^2)/b^2); %second eccentricity
```

%Computing misclosure and design matrix

```
for i=1:N/2;
    m1(i)=-sin(gw(2*i-1))*cos(gw(2*i-1))*X0/rp(i);
    m2(i)=(-sin(gw(2*i))*cos(gw(2*i-1))*Y0+Z0*cos(gw(2*i-1)))/rp(i);
    m3(i)=ew^2*sin(gw(2*i-1))*cos(gw(2*i-1))*da/rp(i)*(sqrt(1-ew^2*sin(gw(2*i-1))^2));
    m4(i)=sin(gw(2*i-1))*cos(gw(2*i-1))*(2/rp(i))*rm(i)+e1^2*(sin(gw(2*i-1)))^2*(1-fw)*df;
    m5(i)=(-X0*sin(gw(2*i))+Y0*cos(gw(2*i)))/(rm(i)*cos(gw(2*i-1)));

    AA(2*i-1,1)=-sin(gw(2*i-1))*cos(gw(2*i-1))/rp(i);
    AA(2*i-1,2)=(-sin(gw(2*i))*cos(gw(2*i-1))+cos(gw(2*i-1)))/rp(i);
    AA(2*i-1,3)=cos(gw(2*i-1))/rp(i);
    AA(2*i,1)=-sin(gw(2*i))/rm(i)*cos(gw(2*i-1));
    AA(2*i,2)=cos(gw(2*i))/rm(i)*cos(gw(2*i-1));
end
```

```
AA=AA*r;
rT1=(m1'+m2'+m3'+m4'/r);
rT2=m5';
for i=1:N/2;.
    rT(2*i-1)=rT1(i);
    rT(2*i)=rT2(i);
end
yy=gd-rT';
```

MOLODENSKY MODEL (3-PARAMETERS)

```

gd=gw-gl;
df=fw-fl;
da=aw-al;

for i=1:N/2
    Vpv(i)=aw/(sqrt(1-ew^2*sin(gw(2*i-1))^2)); %radius in the
                                                prime vertical
    Vmd(i)=aw*(1-ew^2)/(1-ew^2*(sin(gw(2*i-1)))^2)^1.5;%radius
                                                in the meridian direction
end;

rp=Vpv';
rm=Vmd';
b=aw*(1-fw);
e1=sqrt((aw^2-b^2)/b^2); %second eccentricity

%Computing misclosure and design matrix
for i=1:N/2;
    m1(i)=-sin(gw(2*i-1))*cos(gw(2*i-1))*X0/rp(i);
    m2(i)=(-sin(gw(2*i))*cos(gw(2*i-1))*Y0+Z0*cos(gw(2*i-
1)))/rp(i);
    m3(i)=ew^2*sin(gw(2*i-1))*cos(gw(2*i-1))*da/rp(i)*(sqrt(1-
ew^2*sin(gw(2*i-1))^2));
    m4(i)=sin(gw(2*i-1))*cos(gw(2*i-
1))*(2/rp(i))*rm(i)+e1^2*(sin(gw(2*i-1)))^2*(1-fw)*df;
    m5(i)=(-X0*sin(gw(2*i))+Y0*cos(gw(2*i)))/(rm(i)*cos(gw(2*i-
1)));

    AA(2*i-1,1)=-sin(gw(2*i-1))*cos(gw(2*i-1))/rp(i);
    AA(2*i-1,2)=(-sin(gw(2*i))*cos(gw(2*i-1))+cos(gw(2*i-
1)))/rp(i);
    AA(2*i-1,3)=cos(gw(2*i-1))/rp(i);
    AA(2*i,1)=-sin(gw(2*i))/rm(i)*cos(gw(2*i-1));
    AA(2*i,2)=cos(gw(2*i))/rm(i)*cos(gw(2*i-1));
end
AA=AA*r;
rT1=(m1'+m2'+m3'+m4'/r);
rT2=m5';
for i=1:N/2;.
    rT(2*i-1)=rT1(i);
    rT(2*i)=rT2(i);
end
yy=gd-rT';

```

```
%Computing the three-dimensional cartesian coordinates for the
seven points in the global and local systems
```

```
s1=matin('a:\data3m.txt',N,1);
s1=s1/r;
```

```
%Computing the weight matrix
for i=1:N;
    j=i;
    WW(i,j)=1/(s1(i)^2);
end;
```

```
D3P=inv(AA'*WW*AA)*AA'*WW*yy;
X01=X0+D3P(1);    %shift in X
Y01=Y0+D3P(2);    %shift in Y
Z01=Z0+D3P(3);    %shift in Z
```

```
diii=yy-(AA*D3P);
SOOO=(diii'*WW*diii)/(N/2-3);
dpoo=SOOO*inv(AA'*WW*AA);
Dpoo=sqrt(diag(dpoo));
```

```
dX0=Dpoo(1);
dY0=Dpoo(2);
dZ0=Dpoo(3);
```

```
PTT=[X01;Y01;Z01];
```

```
%BURSA-WOLF MODEL (7-PARAMETRS)
```

```
for i=1:7
```

```
c11=3*i-2;
c12=3*i-1;
c13=3*i;
```

```
y3(c11)=X0;
y3(c12)=Y0;
y3(c13)=Z0;
```

```
end;
```

```
y3=y3';
```

```
%computing the misclosures(y)
```

```
y=t-y3;
```

```
%Computing Design matrix
for i=1:7;
```

```
A(3*i-2,1)=1;
A(3*i-2,4)=y2(3*i-2);
A(3*i-2,6)=-y2(3*i);
A(3*i-2,7)=y2(3*i-1);
A(3*i-1,2)=1;
A(3*i-1,4)=y2(3*i-1);
A(3*i-1,5)=y2(3*i);
A(3*i-1,7)=-y2(3*i-2);
A(3*i,3)=1;
A(3*i,4)=y2(3*i);
A(3*i,5)=-y2(3*i-1);
A(3*i,6)=y2(3*i-2);
end;
```

```
s=matin('a:\data3.txt',21,1);
```

```
%Computing the weight matrix
for i=1:21;
```

```
    j=i;
    W(i,j)=1/(s(i)^2);
end;
```

```
for j=1:3;
    y=t-y3;
end
```

```
D=inv(A'*W*A)*A'*W*y;
X0=X0+D(1);    %shift in X;
Y0=Y0+D(2);    %shift in Y;
Z0=Z0+D(3);    %shift in Z;
q=1+D(4);      %scale factor;
THETA1=D(5);   %rotation about the X-axis;
THETA2=D(6);   %rotation about the Y-axis;
THETA3=D(7);   %rotation about the Z-axis;
y4=[X0;Y0;Z0];
```

```
y3=[y4;y4;y4;y4;y4;y4;y4];
```

```
di=y-(A*D);
soo=(di'*W*di)/21-7;
'dp=soo*inv(A'*W*A);
Dp=sqrt(diag(dp));
```

```
rotation1=THETA1*r;
rotation2=THETA2*r;
rotation3=THETA3*r;
```


Standard errors of the parameters

```
dXO=Dp(1);  
dYO=Dp(2);  
dZO=Dp(3);  
dq=Dp(4);  
drot1=Dp(5)*r;  
drot2=Dp(6)*r;  
drot3=Dp(7)*r;
```

```
X=[X0;Y0;Z0;q;THETA1;THETA2;THETA3];
```

```
RC=[1 THETA3 -THETA2;-THETA3 1 THETA1;THETA2 -THETA1 1];
```

rotation matrix

Computating Local 3-D Coordinates from WGS84 (geodetic) Coordinates

```
disp(' ');  
disp(' ');
```

```
disp('ENTER LATITUDE IN DEGREES,MINUTES AND SECONDS AT THE  
PROMPT');
```

```
disp(' ');  
disp(' ');  
Lat1=input('Enter Degrees ');  
Lat2=input('Enter Minutes ');  
Lat3=input('Enter Seconds ');  
disp(' ');  
disp(' ');
```

```
disp('ENTER LONGITUDE IN DEGREES,MINUTES AND SECONDS AT THE  
PROMPT');
```

```
disp(' ');  
disp(' ');  
Long1=input('Enter Degrees ');  
Long2=input('Enter Minutes ');  
Long3=input('Enter Seconds ');  
disp(' ');  
disp(' ');
```

```
r1=[Lat1 Lat2 Lat3;Long1 Long2 Long3];
```

```
%r1=input('Enter latitude and longitude on WGS-84 reference  
ellipsoid ');[ ]
```

Changing from degrees to radians

```
for i=1:2  
    rlr(i)=(r1(i,1)+r1(i,2)/60+r1(i,3)/3600)*pi/180;  
end;
```

```

gww=rlr';

Vvw=aw/(sqrt(1-ew^2*sin(gww(1))^2)); %radius in the prime
vertical
LWX= Vvw*cos(gww(1))*cos(gww(2)); %X
LWY= Vvw*cos(gww(1))*sin(gww(2)); %Y
LWZ= Vvw*(1-ew^2)*sin(gww(1)); %Z

S=[LWX-X0;LWY-Y0;LWZ-Z0];
AS=1/q*RC'*S;

%Computation of local 3-d cartesian coordinates using 3
parameters
SL=[LWX-PTT(1);LWY-PTT(2);LWZ-PTT(3)];
ASL=SL;

%Computing the geodetic coordinates from the cartesian
coordinates

b=a1*(1-f1);
e1=sqrt((a1^2-b^2)/b^2);
e2=(2*f1-f1*f1);
K=0.9996; %UTM Projection Scale factor

p=sqrt((ASL(1))^2+(ASL(2))^2);
theta=atan(ASL(3)*a1/(p*b));
labda=atan(ASL(2)/ASL(1));
PHI=(ASL(3)+(e1^2*b*(sin(theta))^3));
PHII=(p-(e1^2*a1*(cos(theta))^3));
PH=atan(PHI/PHII);
LABDA=labda;

h=-PH;
H=39*pi/180-LABDA;
VO=a1/(sqrt(1-(e2*(sin(h)))^2));
ro=a1*(1-e2)/(sqrt(1-e2*(sin(h))^2))^3;

n=f1/(2-f1);
co=1+n^2/4+n^4/64;
c12=3/2*(n-n^3/8);
c14=15/16*(n^2-n^4/4);
c16=35/48*n^3;
c18=315/512*n^4;
so=a1/(1+n)*(co*h-c12*sin(2*h)+c14*sin(4*h)-
c16*sin(6*h)+c18*sin(8*h));

```

```

Nl1=((VO/2)*(H*cos(h))^2*tan(h))+((VO/24)*(H*cos(h))^4*tan(h)*
(5-(tan(h))^2));
NL1=10000000-K*(so+NL1);
EL1=500000-K*((VO*H*cos(h))+((VO/6)*(H*cos(h))^3)*((VO/ro)-
(tan(h))^2))+((VO/120)*(H*cos(h))^5*(5-
18*(tan(h))^2+(tan(h))^4));

```

```

eh=input('Enter ellipsoidal height ');
Lc=[NL1;EL1;eh];

```

```

%Reading plane coordinates on the local grid(Arc-Datum,1960)
and Orthometric height from %data file data4.txt.

```

```

p=matin('a:\data4.txt',14,3);
n0=size(p);
KK=n0(1);
PP=n0(2);
n=KK;

```

```

%Computing design matrix
for i=1:KK;
A1(i,1)=1;
A1(i,2)=p(i,1);
A1(i,3)=p(i,2);
A1(i,4)=p(i,1)*p(i,2);
A1(i,5)=(p(i,1))^2;
A1(i,6)=p(i,2)^2;
A1(i,7)=(p(i,1))^2*p(i,2);
A1(i,8)=p(i,1)*(p(i,2))^2;
A1(i,9)=(p(i,1))^2*(p(i,2))^2;
HT(i,1)=p(i,PP);

```

```

end;

```

```

%Reading standard errors from data file (data5.txt)
s2=matin('a:\data5.txt',14,1);

```

```

%Computing the weight matrix
C01=0;
for i=1:14;
j=i;
W1(i,j)=1/(s2(i)^2);
C01=C01+s2(i)^2;

```

```

end;
k=inv(A1'*W1*A1)*(A1'*W1*HT);
k0=k(1);
k1=k(2);k2=k(3);k3=k(4);k4=k(5);k5=k(6);k6=k(7);k7=k(8);
k8=k(9);

```

```
%Computation of geoidal undulation at a given point
```

```
N=k0+k1*Lc(1)+k2*Lc(2)+k3*Lc(1)*Lc(2)+k4*(Lc(1))^2+k5*(Lc(2))^2+k6*(Lc(1))^2*Lc(2)+k7*Lc(1)*(Lc(2))^2+k8*(Lc(1))^2*(Lc(2))^2;
```

```
%LEAST SQUARES COLLOCATION COMPUTATIONS
```

```
%Approximation of the covariance constants
```

```
C0=C01/14;  
cont=0.01;  
cont1=cont^2;  
a111=cont1/C0;  
a1111=log(a111);  
a11111=sqrt(-1*(a1111));  
a=a11111/1000000; %approximated by interpretation and scaled
```

```
%Computation of Signal part of the Observations
```

```
for i=1:n;
```

```
d1(i,1)=sqrt((p(i,1)-p(1,1))^2+(p(i,2)-p(1,2))^2);  
d2(i,1)=sqrt((p(i,1)-p(2,1))^2+(p(i,2)-p(2,2))^2);  
d3(i,1)=sqrt((p(i,1)-p(3,1))^2+(p(i,2)-p(3,2))^2);  
d4(i,1)=sqrt((p(i,1)-p(4,1))^2+(p(i,2)-p(4,2))^2);  
d5(i,1)=sqrt((p(i,1)-p(5,1))^2+(p(i,2)-p(5,2))^2);  
d6(i,1)=sqrt((p(i,1)-p(6,1))^2+(p(i,2)-p(6,2))^2);  
d7(i,1)=sqrt((p(i,1)-p(7,1))^2+(p(i,2)-p(7,2))^2);  
d8(i,1)=sqrt((p(i,1)-p(8,1))^2+(p(i,2)-p(8,2))^2);  
d9(i,1)=sqrt((p(i,1)-p(9,1))^2+(p(i,2)-p(9,2))^2);  
d10(i,1)=sqrt((p(i,1)-p(10,1))^2+(p(i,2)-p(10,2))^2);  
d11(i,1)=sqrt((p(i,1)-p(11,1))^2+(p(i,2)-p(11,2))^2);  
d12(i,1)=sqrt((p(i,1)-p(12,1))^2+(p(i,2)-p(12,2))^2);  
d13(i,1)=sqrt((p(i,1)-p(13,1))^2+(p(i,2)-p(13,2))^2);  
d14(i,1)=sqrt((p(i,1)-p(14,1))^2+(p(i,2)-p(14,2))^2);
```

```
t1=-(a^2*d1(i,1)^2);  
t2=-(a^2*d2(i,1)^2);  
t3=-(a^2*d3(i,1)^2);  
t4=-(a^2*d4(i,1)^2);  
t5=-(a^2*d5(i,1)^2);  
t6=-(a^2*d6(i,1)^2);  
t7=-(a^2*d7(i,1)^2);  
t8=-(a^2*d8(i,1)^2);  
t9=-(a^2*d9(i,1)^2);  
t10=-(a^2*d10(i,1)^2);  
t11=-(a^2*d11(i,1)^2);  
t12=-(a^2*d12(i,1)^2);  
t13=-(a^2*d13(i,1)^2);  
t14=-(a^2*d14(i,1)^2);
```

```

Css1(i,1)=C0*exp(t1);
Css2(i,1)=C0*exp(t2);
Css3(i,1)=C0*exp(t3);
Css4(i,1)=C0*exp(t4);
Css5(i,1)=C0*exp(t5);
Css6(i,1)=C0*exp(t6);
Css7(i,1)=C0*exp(t7);
Css8(i,1)=C0*exp(t8);
Css9(i,1)=C0*exp(t9);
Css10(i,1)=C0*exp(t10);
Css11(i,1)=C0*exp(t11);
Css12(i,1)=C0*exp(t12);
Css13(i,1)=C0*exp(t13);
Css14(i,1)=C0*exp(t14);

end;
cov=[Css1';Css2';Css3';Css4';Css5';Css6';Css7';Css8';Css9';Css
10';Css11';Css12'; Css13'; Css14'];

%Computation of Cross Covariance from Signal to Observation
Points
%Reading plane coordinates of interpolation points from data
file
p1=matin('a:\data6.txt',5,2);

for i=1:n;
d11(i,1)=sqrt((p(i,1)-p1(1,1))^2+(p(i,2)-p1(1,2))^2);
d12(i,1)=sqrt((p(i,1)-p1(2,1))^2+(p(i,2)-p1(2,2))^2);
d13(i,1)=sqrt((p(i,1)-p1(3,1))^2+(p(i,2)-p1(3,2))^2);
d14(i,1)=sqrt((p(i,1)-p1(4,1))^2+(p(i,2)-p1(4,2))^2);
d15(i,1)=sqrt((p(i,1)-p1(5,1))^2+(p(i,2)-p1(5,2))^2);

t11=-(a^2*d11(i,1)^2);
t12=-(a^2*d12(i,1)^2);
t13=-(a^2*d13(i,1)^2);
t14=-(a^2*d14(i,1)^2);
t15=-(a^2*d15(i,1)^2);

Css11(i,1)=C0*exp(t11);
Css12(i,1)=C0*exp(t12);
Css13(i,1)=C0*exp(t13);
Css14(i,1)=C0*exp(t14);
Css15(i,1)=C0*exp(t15);

end;

```

```

cov1=[Css11';Css12';Css13';Css14';Css15'];

%Computation of Covariances for the random part (cov2)

for i=1:5;
d111(i,1)=sqrt((p1(i,1)-p1(1,1))^2+(p1(i,2)-p1(1,2))^2);
d112(i,1)=sqrt((p1(i,1)-p1(2,1))^2+(p1(i,2)-p1(2,2))^2);
d113(i,1)=sqrt((p1(i,1)-p1(3,1))^2+(p1(i,2)-p1(3,2))^2);
d114(i,1)=sqrt((p1(i,1)-p1(4,1))^2+(p1(i,2)-p1(4,2))^2);
d115(i,1)=sqrt((p1(i,1)-p1(5,1))^2+(p1(i,2)-p1(5,2))^2);

t111=-(a^2*d111(i,1)^2);
t112=-(a^2*d112(i,1)^2);
t113=-(a^2*d113(i,1)^2);
t114=-(a^2*d114(i,1)^2);
t115=-(a^2*d115(i,1)^2);

Css111(i,1)=C0*exp(t111);
Css112(i,1)=C0*exp(t112);
Css113(i,1)=C0*exp(t113);
Css114(i,1)=C0*exp(t114);
Css115(i,1)=C0*exp(t115);

end;

cov2=[Css111';Css112';Css113';Css114';Css115'];

%Computation of the Diagonal Matrix(Cnn)
for i=1:14;
    j=i;
    Cnn(i,j)=s2(i)^2;
end

C11=Cnn+cov;

sol=inv(A1'*inv(C11)*A1);
Psol=sol*A1'*inv(C11)*HT;
Sig=cov1*inv(C11)*(HT-A1*Psol);

%Computation of Design Matrix of Signal Points

for i=1:5;
A2(i,1)=1;
A2(i,2)=p1(i,1);
A2(i,3)=p1(i,2);
A2(i,4)=p1(i,1)*p1(i,2);
A2(i,5)=(p1(i,1))^2;
A2(i,6)=p1(i,2)^2;
A2(i,7)=(p1(i,1))^2*p1(i,2);

```

```

A2(i,8)=p1(i,1)*(p1(i,2))^2;
A2(i,9)=(p1(i,1))^2*(p1(i,2))^2;

end;

%COMPUTATION OF THE SIGNALS
gh=A2*Psol+Sig;
H=eh-N;
% COMPUTATION OF THE STANDARD ERRORS OF THE COEFFICIENTS(LS)
td=HT-(A1*k);
SOO=(td'*W1*td)/5;
stdc=inv(A1'*W1*A1)*SOO;

stdLS=sqrt(diag(stdc));

% COMPUTATION OF THE STANDARD ERRORS OF THE COEFFICIENTS(LSC)
STDC=inv(A1'*inv(C11)*A1);
stdLSC=sqrt(diag(STDC));
%COMPUTATION OF THE STANDARD ERRORS OF THE SIGNALS(LSC)
ach=A1*inv(A1'*inv(C11)*A1)*A1'*inv(C11);
for i=1:14;
    I(i,i)=1;
end;
STDS=cov2-cov1*inv(C11)*(I-ach)*cov1';
stdS=sqrt(diag(STDS));

%DISPLAYING RESULTS
disp(' ');
disp(' ');
disp('RESULTS');
disp(' ');
disp(' ');
format bank
disp('Northing Value in m ');Lc(1)
disp('-----')
disp('Easting Value in m ');Lc(2)
disp('-----')
disp('Geoidal height in m ');N
disp('-----')
disp('Orthometric height in m ');H
disp('*****')
disp('*****')

```

```

disp('SUMMARY OF THE COMPUTATIONS');
disp('-----')

disp('      Northing(m)      Easting(m)      Orthometric
height(m)');
      [Lc(1)      Lc(2)      H]
disp('*****')
disp('*****')
disp('      ');
disp('Thank you Odera,P.A')
disp('      ');
disp('      ');
disp('Please type the word [RUN] to continue or [exit] to
discontinue')
disp('      ');
disp('      ');

```


APPENDIX C: USER INTERFACE

» RUN

This program determines: transformation parameters, polynomial coefficients, geoid heights, local plane coordinates and orthometric heights.

By Patroba, A. Odera.

USER INTERFACE

PLEASE ENJOY THE PROGRAM

THE USER IS REQUIRED TO INPUT THE RIGHT DATA AT THE PROMPT

PLEASE USE THE RIGHT FORMAT AS INDICATED

INPUT-LATITUDE (-ve if S), LONGITUDE AND ELLIPSOIDAL HEIGHT ON WGS84

OUTPUT-N,E ON ARC DATUM1960,GEOID HEIGHT AND ORTHOMETRIC HEIGHT

INPUT DATA

ENTER LATITUDE IN DEGREES, MINUTES AND SECONDS AT THE PROMPT

Enter Degrees -1
Enter Minutes -24
Enter Seconds -7.26869

ENTER LONGITUDE IN DEGREES, MINUTES AND SECONDS AT THE PROMPT

Enter Degrees 36
Enter Minutes 56
Enter Seconds 40.17275

Enter ellipsoidal height 1573.3818

RESULTS

Northing Value in m

9845232.61

Easting Value in m

271195.98

Geoidal height in m

N = -16.83

Orthometric height in m

H = 1590.21

SUMMARY OF THE COMPUTATIONS

Northing (m) Easting (m) Orthometric height (m)

9845232.61 271195.98 1590.21

Thank you: Odera, P.A

Please type the word [RUN] to continue or [EXIT] to discontinue.

»

N/B: The point Stigands X has been used in this User Interface as an example.

REFERENCES

- Allman, J.S. and Veenstra, C., (1982). Geodetic models of Australia, Department of Resources and Energy Division of National Mapping, Australia.
- Anderle, R.J., (1966). Geodetic parameters set NWL-SE-6 based on Doppler Satellite Observations. Proceedings of the second International Symposium of Geodesy, Athens, Greece.
- Arabelos, D., (1989). Gravity field approximation in the area of Greece with emphasis on local characteristics. Bull. Geoid. Volume 63, No.1, pp. 69 – 84.
- Aseno, J.O., Mahinda, J.N. and Munene, C.M., (1994). “ The need for accurate horizontal controls to facilitate deformation monitoring in Kenya”. Paper presented at the fourth International Symposium on Recent Crustal Movements in Africa, held in Nairobi, Kenya, November 28- December 2, 1994.
- Ayhan, M.E., (1993). Geoid determination in Turkey, Bulletin Géodésique, Volume 67, No.1, Feb 1993, pp. 10 – 22.
- Bowring, R.B., (1978). The Surface Controlled Spatial System for Computations, Survey Review, Volume 24, No. 190, pp. 361 – 372.
- Davis, P.J., (1975). Interpolation and Approximation, New York, United States of America.
- Denker, H., Torge, W., Wenzel, G., Lelgeman, D. and Weber, G., (1986). Strategies and requirements for a new European geoid computations. Proceedings of the International Symposium on the Definition of the Geoid, May 26 – 30, Florence.
- Doerflinger, E., Jiang, Z., Duquenne, H. and Bayer, R., (1997). Determination of the quasi – geoid in a mountainous area, example of eastern Pyrenees (France). In “Gravity, Geoid and Marine Geodesy.” pp. 643 – 650, Springer.
- Featherstone, W.E., Dentith, M.C. and Kirby, J.F., (1998). Strategies for the accurate determination of orthometric heights from GPS. Survey Review, Volume 34, No. 267, pp. 278 – 296.
- Gill, D., (1896). Report on the geodetic survey of South Africa, Government printer, Cape Town.
- Guier, W.U. and Newton, R.R., (1965). The Earth's gravity field deduced from the Doppler tracking of five satellites. Journal of Geophysical Research, pp. 4613 – 4626.
- Heiskanen, W.A. and Moritz, H., (1967). Physical Geodesy, Freeman and Company, San Francisco.
- Hofmann-Wellenhof, B.H., Lichtenegger, H. and Collins, J., (1992). “Global Positioning System, Theory and Practice.” Springer – Verlag, Wien, New York.

- Izsak, I.G., (1966). A new determination of non – zonal harmonics by satellites Trajectories of Artificial Celestial Bodies as Determined from Observations, Springer – Verlag, Berlin.
- Kaula, W., (1966 b). Test and combination of satellite determination of gravity field with gravimetry. *Journal of Geophysics*, No. 71, pp. 5303 – 5314.
- Kearsley, A.H.W. and Forsberg, R., (1990). Tailored geopotential models applications and shortcomings, *Manuscripta Geodetica*, Volume 15, No. 3, pp. 151 – 158.
- Kozai, Y., (1959). The Earth's gravitational potential derived from the motion of satellite, Special Report No. 22.
- Kozai, Y., (1964). New determination of zonal harmonic coefficients in the Earth's gravitational potential. *Publ. Astron. Soc. Jpn.* 16.
- Krarup, T., (1969). Contribution to the mathematical formulation of physical geodesy, Danish Geodetic Institute, No. 44, Copenhagen.
- Lachapelle, G. and Tscherning, C.C., (1978). Use of Collocation for predicting geoid Undulations and related quantities over large areas. *Proceedings of the International Symposium on the geoid in Europe and Mediterranean Area*, Ancona, pp. 133 – 152.
- Langley, R. B., (1992). Basic Geodesy for GPS, *Innovation, GPS World*, February 1992. pp. 44 – 48.
- Leick, A., (1990). *GPS Satellite Surveying*, John Willey and Sons, New York.
- Lwangasi, A.S., (1991). Free – Air Gravity Anomalies in Kenya, *International Association of Geodesy Symposia*, 1991, pp. 261 – 267.
- Magnavox Research Laboratory Report No. MX – TR – 2027 – 72, January 1972.
- Maling, D.H., (1973). *Coordinate Systems and Map Projections*. Philip, London, England.
- Merry, C.L., (1978). A note on the geoidal heights in South Africa. *Survey Review*, Volume 24, No. 189.
- Moritz, H., (1973). Determination of gravity field by collocation, Report No.32, pp. 1- 12.
- Moritz, H., (1980). *Advanced Physical Geodesy*, Abacus Press, London, England.
- Mueller, I.I., (1991). Planning an International Service using the Global Positioning System for Geodynamic Applications. "Permanent Satellite Tracking Networks for Geodesy and Geodynamics". *International Association of Geodesy, Symposium No 109*, Vienna, Austria, August 11 – 24, 1991. pp. 1 – 22.
- Mwakuchengwa, B.M., (1994). " On the Kenyan Geodetic datum: Need for a new geodetic datum for precise geodetic projects". Paper presented at the fourth International Symposium on Recent Crustal Movements in Africa. Nairobi, Kenya. November 28 — December 2, 1994.

- Pan, M. and Sjöberg, L.E., (1998). Unification of vertical datums by GPS and gravimetric geoid models with application to Fennoscandia, *Journal of Geodesy*, Volume 72, No 2, February 1998. pp. 64 – 70.
- Pizer, S.M., (1975). *Numerical Computing and Mathematical analysis*, Department of Computer Science, University of North Carolina, Charpel Hill, N.C.
- Rapp, R.H., (1986). Global potential solutions. (In: *mathematical numerical techniques in physical geodesy*. Edited by Sünkel, H), Springer Verlag, pp. 365 – 415.
- Rapp, R.H. and Balasubramania, N., (1992). A conceptual formulation of a world height system, Department of Geodetic Sciences, Report No. 421, Ohio State University, Columbus, Ohio, United States of America.
- Rapp, R.H., (1997). Global models for the 1cm geoid – present status near term prospects. (In: *geodetic boundary value problem in view of the one-centimeter geoid*. Edited by Sanso, F and Rummel, R), Springer Verlag.
- Rainsford, H.F., (1951). The African Arc of the 30th Meridian. *Emperor Survey Review*, No. XI, pp. 159 – 163.
- Rens, J. and Merry, C.L., (1990). Datum transformation in South Africa. *Survey Review*, Volume 30, No. 236, pp. 281 – 293.
- Resch, G.M., (1984). Water Vapor radiometry in geodetic applications, *Geodetic Refraction*, Springer-Verlag, pp. 85 – 141.
- Rizos, C., (1980). The role of the gravity field in sea surface topography studies, PhD thesis, School of Surveying, University of New South Whales, Australia.
- Rogers, H.H.M., (1982). The re-adjustment of the trigonometrical controls in North Eastern Kenya. Technical report, Survey of Kenya.
- Santere, R., (1989). GPS Satellite Sky Distribution: Impact on the propagation of some Important Errors in Precise Relative Positioning. Department of Surveying Engineering, University of New Brunswick, Fredericton, N.B, Canada, Technical Report No. 145.
- Schwarz, K.P. and Sideris, M.G., (1985). Precise geoid heights and their use in GPS interferometry. Geodetic Survey of Canada, Department of Energy, Mines and Resources, Ottawa.
- Schwarz, K.P., Sideris, M.G. and Forsberg, R., (1987). Orthometric heights without leveling, *Journal of Surveying Engineering*, Volume 113, No. 1, pp. 28 – 40.
- Sideris, M.G. and Schwarz, K.P., (1986). Improvement of medium and short wavelength features of geopotential solutions by local data. Proceedings of the International Symposium on the definition of the Geoid, May 26 – 30, Florance.

Sünkel, H., Bartelme, N., Fuchs, H., Hamafy, M. and Schuh, W.D., (1987). The gravity field in Australia. IUGG XIX General Assembly. Proceedings of the IAG Symposium. Volume 2, pp. 475 – 503.

Torge, W., (1980). Geodesy, Walter de Gruyter-Berlin, New York.

Torge, W., Basic, T., Denker, H., Dolift, I. and Wenzel, G., (1989). Long range geoid control through the European GPS traverse, DGK, Reihe B, Heft Nr. 290.

Torge, W., (1991). Geodesy, second edition, Walter de Gruyter-Berlin, New York.

Uren, J. and Price, W.F., (1994). Surveying for Engineers, Macmillan, Britain.

Vaniček, P. and Klausberg., (1987). The Canadian geoid Stokesian approach. Manuscripta Geodetica, Vol 12, No.2, pp. 86 – 98.

Vaniček, P., (1973). Gravimetric satellite Geodesy, Department of Surveying Engineering, University of New Brunswick, Canada.

Yang, Z.J. and Chen, Y.Q., (1999). Determination of local geoid with the geometric method – a case study, Journal of Surveying Engineering, Volume 125, No. 3, pp.136 – 146.

Yang, Z.J. and Chen, Y.Q., (2002). A hybrid method to determine Hong Kong geoid, Hong Kong, China.

Weber, G. and Zomorrodian, H., (1988). Regional geopotential model improvement for the Iranian geoid determination. Bulletin of Geodesy, Volume 62, No.2, pp. 125 – 145.

www.nima.mil/GrandG/wgsegm/egm96.html.

UNIVERSITY OF NAIROBI
EAST AFRICANA COLLECTION

JON

WALTER A. WELLS
LIBRARY